FOSSIL ENERGY

DOE/BC/15026-1
(OSTI ID: 756282)

LOCATION, REPROCESSING, AND ANALYSIS OF TWO DIMENSIONAL SEISMIC REFLECTION DATA ON THE JICARILLA APACHE INDIAN RESERVATION, NEW MEXICO

Final Report
September 1, 1997-February 1, 2000

By:
Jennie Ridgley
David J. Taylor
A. Curtis Huffman, Jr.

Date Published: April 2001

Work Performed Under Contract No. DE-FG26-98BC15026

U.S. Geological Survey
Denver, Colorado

National Energy Technology Laboratory
National Petroleum Technology Office
U.S. DEPARTMENT OF ENERGY
Tulsa, Oklahoma

DOE/BC/15026-1
Distribution Category UC-122

Location, Reprocessing, and Analysis of Two Dimensional Seismic Reflection Data on the Jicarilla Apache Indian Reservation, New Mexico

By
Jennie Ridgley
David J. Taylor
A. Curtis Huffman, Jr.

April 2001

Work Performed Under Contract DE-FG26-98BC15026

Prepared for
U.S. Department of Energy
Assistant Secretary for Fossil Energy

Ginny Weyland, Project Manager
National Petroleum Technology Office
P.O. Box 3628
Tulsa, OK 74101

Prepared by
U.S. Geological Survey
MS 939 Box 25046 DFC
Denver, CO 80225

Table of Contents

List of Figures

List of Tables

List of Plates

Abstract

Multichannel surface seismic reflection data recording is an standard industry tool used to examine various aspects of geology, especially the stratigraphic characteristics and structural style of sedimentary formations in the subsurface. With the help of the Jicarilla Apache Tribe and the Bureau of Indian Affairs we were able to locate over 800 kilometers (500 miles) of multichannel seismic reflection data located on the Jicarilla Apache Indian reservation. Most of the data was recieved in hardcopy form, but there were data sets where either the demultiplexed digital field data or the processed data accompanied the hardcopy sections. The seismic data was acquired from the mid 1960's to the early 1990's. The most extensive seismic coverage is in the southern part of the reservation, although there are two good surveys located on the northeastern and northwestern parts of the reservation. Most of the data show that subsurface formations are generally flat-lying in the southern and western portion of the reservation. There is, however, a significant amount of structure imaged on seismic data located over the San Juan Basin margin along the east-central and northern part of the reservation. Several west to east trending lines in these areas show a highly faulted monoclinal structure from the deep basin in the west up onto the basin margin to the east. Hydrocarbon exploration in flat lying formations is mostly stratigraphic in nature. Where there is structure in the subsurface and indications are that rocks have been folded, faulted, and fractured, exploration has concentrated on structural traps and porosity/permeability "sweet spots" caused by fracturing. Therefore, an understanding of the tectonics influencing the entire section is critical in understanding mechanisms for generating faults and fractures in the Cretaceous.

It is apparent that much of the hydrocarbon production on the reservation is from fracture porosity in either source or reservoir sequences. Therefore it is important to understand the mechanism that controls the location and intensity of the fractures. A possible mechanism may be deep seated basement faulting that has been active through time. Examining the basement fault patterns in this part of the basin and their relation to fracture production may provide a model for new plays on the Jicarilla Indian Reservation. There are still parts of the reservation where the subsurface has not been imaged geophysically with either conventional two-dimensional or three-dimensional reflection seismic techniques. These methods, especially 3-D seismic, would provide the best data for mapping deep basement faulting. The authors would recommend that 3-D seismic be acquired along the Basin margin located along the eastern edge of the reservation and the results be used to construct detailed fault maps which may help to locate areas with the potential to contain highly fractured zones in the subsurface.

Introduction

Exploration for oil and gas by both large and small companies has taken place in northern part of the San Juan Basin in New Mexico, including the Jicarilla Apache reservation, for many years. As part of their exploration efforts various companies acquired a significant amount of two-dimensional multichannel seismic reflection data on both regional and prospect scales. The primary purpose of this study was to locate and collect as much of this seismic data as possible, bringing it into a central location where it could be evaluated, reprocessed, and interpreted. The interpretation provides additional subsurface structural information valuable in support of traditional geologic mapping using well log data.

Working with the Jicarilla Indian Tribe and the Bureau of Indian Affairs we were able to locate and acquire, at no cost to the project, a grid of two-dimensional seismic data over much of the reservation. The data were gathered and stored at the U.S. Geological Survey offices in Denver, Colorado, where project scientists could work with the data. In most cases, only paper and/or film copies of the seismic sections could be acquired. A few lines were received in either digital unprocessed and/or processed form and did accompany the hardcopy materials. Reprocessing of a sample of the digital field data confirmed the quality of the hardcopy sections and produced digital output which were then available to load into an interpretation workstation

Interpretation of selected lines in the database provided a general structural depiction of the subsurface. Sonic measurements from several key wells adjacent to the seismic lines were used to generate synthetic seismograms and enabled the interpreters to correlate geologic formations with specific events on the seismic sections. Examination of the structural patterns for these key events contributed to the overall structural interpretation, fault alignment, and tectonic history.

Results and Discussion

Multichannel Reflection Seismic Data Resources

This project had no funding for new seismic field acquisition or acquisition of previously shot data from commercial data brokers. This narrowed the search to data that the Jicarilla Apache Tribe could provide through seismic acquisition permit agreements with companies doing business on the reservation. After inquiring with the Tribe it was determined that a significant amount of seismic data had been transferred to the Bureau of Indian Affairs (BIA) Division of Energy and Mineral Resources office in Lakewood, Colorado. Arrangements were made to transfer this entire seismic database to the U.S. Geological Survey Central Energy Resources Team office in Lakewood, Colorado. The Jicarilla Tribe also supplied seismic data held at the tribal headquarters in Dulce, New Mexico.

The project was able to collect 882.5 km (548.2 miles) of multichannel seismic reflection data located on the Reservation. The database acquired from the BIA and the Tribe included digital seismic shotpoint files in SEGP1 format. Using GeoGraphix GES software, a map showing the location of the seismic lines and shotpoints derived from the SEGP1 digital location files was generated (Plate 1). Plate 1 shows that the majority of the seismic data lies over the southern portion of the reservation. These seismic surveys were acquired for Amoco Production Company, Texaco, Conoco, Meridian Oil Company, and the Tenneco Oil Company. There are two good recently acquired high quality seismic surveys located further north. These were acquired for the American Hunter Oil Company and Southland Royalty. Table 1 is a list of seismic lines making up the final database collected by the U.S. Geological Survey for this project.

Generally, the quality of the seismic data in the database is good. This is especially true for the data that was acquired within the last ten years. These modern surveys tended to use more recording channels with acquisition parameters resulting in higher fold data. Higher fold usually results in a better signal to noise ratio and produces more coherent looking data. The surveys for American Hunter Oil Company, and Conoco/Meridian oil companies have stacking folds of 3000% (30 fold) to 6000% (60 fold) (see table 1). The Southland Royalty data is also relatively high fold at 2400% (24 fold), but the data shot for Amoco and Texaco is low fold at 600% (6 fold). The 600% data was shot in areas that were not structurally complex rather than over the highly folded, faulted and fractured areas along the San Juan Basin margin. Figure 1 shows the difference between 4000% (40 fold) data from Conoco/Meridian compared to 600% (6 fold) data shot for Texaco in roughly the same area. Note that the 40 fold data from Conoco/Meridian on the left contains sharper and more numerous reflections than the 6 fold data from Texaco on the right. Both where shot using a dynamite source and used an acquisition and processing sample interval of 2 milliseconds.

With the exception of the Southland Royalty data most of the data was acquired using a dynamite source. The Southland Royalty data used vibrators as the energy source. Dynamite tends to induce higher frequencies into the subsurface

Table 1. - Seismic Coverage

Company	Line No.	Date Shot	Date Proc	Source	Fold	Miles
American Hunter	J-1-91	Aug-91	Oct-91	Dynamite	30	9.8
American Hunter	J-3-91	Aug-91	Oct-91	Dynamite	30	2.0
American Hunter	J-4-91	Sep-91	Oct-91	Dynamite	30	3.7
American Hunter	J-5-91	Sep-91	Oct-91	Dynamite	30	5.8
American Hunter	J-6-92	Jun-92	Jul-92	Dynamite	30	5.7
American Hunter	J-7-92	Jun-92	Jul-92	Dynamite	30	6.6
American Hunter	J-8-92	Jun-92	Jul-92	Dynamite	30	6.9
American Hunter	J-9-92	Jun-92	Jul-92	Dynamite	30	5.6
American Hunter	J-14-93	Jul-94	Dec-94	Dynamite	50	6.0
American Hunter	J-15-93	Jul-94	Dec-94	Dynamite	60	3.7
American Hunter	J-16-93	Jul-94	Dec-94	Dynamite	60	5.6
American Hunter	J-17-93	Jul-94	Dec-94	Dynamite	60	4.8
American Hunter	J-18-93	Jul-94	Dec-94	Dynamite	60	4.4
American Hunter	J-19-93	Jul-94	Dec-94	Dynamite	60	5.9
American Hunter	J-20-93	Jul-94	Dec-94	Dynamite	60	6.4
American Hunter	J-21-93	Jul-94	Dec-94	Dynamite	60	6.4
American Hunter	J-22-93	Jul-94	Dec-94	Dynamite	60	3.1
American Hunter	J-23-93	Jul-94	Dec-94	Dynamite	60	3.3
American Hunter	J-24-93	Jul-94	Dec-94	Dynamite	60	3.4
American Hunter	J-25-93	Jul-94	Dec-94	Dynamite	60	4.0
						103.1
Southland Royalty	84-1	Jun-84	Sep-84	Vibroseis	24	10.5
Southland Royalty	84-2	Jul-84	Sep-84	Vibroseis	24	8.7
Southland Royalty	84-3	Jun-84	Sep-84	Vibroseis	24	5.9
Southland Royalty	84-4	Jun-84	Sep-84	Vibroseis	24	6.6
Southland Royalty	84-5	Jun-84	Sep-84	Vibroseis	24	6.5
Southland Royalty	84-6	Jun-84	Sep-84	Vibroseis	24	6.4
Southland Royalty	84-7	Jul-84	Sep-84	Vibroseis	24	5.0
						49.6
Conoco/Meridian	MOICON 8A	Sep-96	3/97 & 2/99	Dynamite	40	15.2
Conoco/Meridian	MOICON 8B	Sep-96	3/97 & 2/99	Dynamite	40	6.3
Conoco/Meridian	MOICON 9A	Sep-96	3/97 & 2/99	Dynamite	40	7.2
Conoco/Meridian	MOICON 9B	Sep-96	3/97 & 2/99	Dynamite	40	7.5
Conoco/Meridian	MOICON 10	Oct-96	3/97 & 2/99	Dynamite	40	6.5
Conoco/Meridian	MOICON 12	Mar-96	Mar-97	Dynamite	40	12.8
						55.5
Meridian	MOI-NTPRDG-93-1	Mar-94	Apr-94	Dynamite	40	5.7
Meridian	MOI-NTPRDG-93-2	Mar-94	Apr-94	Dynamite	40	5.1
Meridian	MOI-BDHL-92-1	Apr-94	Apr-94	Dynamite	40	1.4
Meridian	MOI-BDHL-92-2	Apr-94	Apr-94	Dynamite	40	3.0
						15.2
Amoco	GDD-A1	N/A	May-66	Dynamite	6	8.1
Amoco	GDD-A2	N/A	Feb-76	Dynamite	6	8.4
Amoco	GDD-AA	N/A	Feb-76	Dynamite	6	7.0
Amoco	GDD-B	N/A	May-66	Dynamite	6	17.1
Amoco	GDD-BB	N/A	Feb-76	Dynamite	6	4.0
Amoco	GDD-C	N/A	May-66	Dynamite	6	Duplicate
Amoco	GDD-C	N/A	Feb-76	Dynamite	6	11.4
Amoco	GDD-CC	N/A	Feb-76	Dynamite	6	4.1

Amoco	GDD-D1	N/A	May-66	Dynamite	6	4.4
Amoco	GDD-D2	N/A	Feb-76	Dynamite	6	7.7
Amoco	GDD-DD	May-66	Feb-76	Dynamite	6	4.6
Amoco	GDD-EE	N/A	Jul-87	Vibroseis	6	No Loc
Amoco	GDD-E3	N/A	Feb-76	Dynamite	6	7.5
Amoco	GDD-K	N/A	Feb-76	Dynamite	6	16.5
Amoco	GDD-L	N/A	Feb-76	Dynamite	6	16.7
Amoco	GDD-M	N/A	Feb-76	Dynamite	6	11.4
Amoco	GDD-N	N/A	N/A	Dynamite	6	4.8
Amoco	GDD-T	N/A	N/A	Dynamite	6	3.6
Amoco	GDD-U	N/A	Feb-76	Dynamite	6	14.1
Amoco	GDD-V	N/A	Feb-76	Dynamite	6	15.7
Amoco	GDD-W	N/A	Feb-76	Dynamite	6	Duplicate
Amoco	GDD-W	Jul-66	Jan-92	Dynamite	24	20.0
Amoco	GDD-X	N/A	Feb-76	Dynamite	6	3.8
Amoco	GDD-Y1	N/A	N/A	N/A	N.A	4.8
Amoco	GDD-Y2	N/A	Feb-76	Dynamite	6	1.9
Amoco	GDD-Z	N/A	Feb-76	Dynamite	6	5.2
Amoco	EE-3	Jul-69	N/A	Vibroseis	6	4.4
Amoco	EE-4	N/A	N/A	N/A	N.A	38.0
Amoco	EE-5	Sep-69	N/A	Vibroseis	6	13.3
						258.5
Texaco	19	Oct-74	Nov-74	Dynamite	6	3.5
Texaco	20	Oct-74	Nov-74	Dynamite	6	3.7
Texaco	22	Oct-74	Nov-74	Dynamite	6	No Loc
Texaco	21	Oct-74	Nov-74	Dynamite	6	4.0
Texaco	23	Oct-74	Nov-74	Dynamite	6	4.9
Texaco	34	Feb-72	Feb-75	Dynamite	6	3.4
Texaco	35	Apr-75	Apr-75	Dynamite	6	3.3
Texaco	538	Nov-75	Nov-75	Dynamite	6	5.2
Texaco	539	Nov-75	Nov-75	Dynamite	6	16.7
Texaco	540	Nov-75	Nov-75	Dynamite	6	19.7
Texaco	546	Dec-75	Dec-75	Dynamite	6	1.9
						66.3
Total Miles						***548.2***

Table 2. - Seismic History

Company	Line	Processing	Copy	Datum (ft)	Vel (ft/sec)
American Hunter	J-1-91	Stk & Mig	Dig./Paper	7000	9000
American Hunter	J-3-91	Stk & Mig	Dig./Paper	7000	9000
American Hunter	J-4-91	Stk & Mig	Paper	7000	9000
American Hunter	J-5-91	Stk & Mig	Dig./Paper	7000	9000
American Hunter	J-6-92	Stk & Mig	Dig./Paper	7000	9000
American Hunter	J-7-92	Stk & Mig	Paper	7000	9000
American Hunter	J-8-92	Stk & Mig	Paper	7000	9000
American Hunter	J-9-92	Stk & Mig	Paper	7000	9000
American Hunter	J-14-93	Stk & Mig	Paper	7000	9000
American Hunter	J-15-93	Stk & Mig	Paper	7000	9000
American Hunter	J-16-936	Stk & Mig	Paper	7000	9000
American Hunter	J-17-93	Stk & Mig	Paper	7000	9000
American Hunter	J-18-93	Stk & Mig	Paper	7000	9000
American Hunter	J-19-93	Stk & Mig	Paper	7000	9000
American Hunter	J-20-93	Stk & Mig	Paper	7000	9000

American Hunter	J-21-93	Stk & Mig	Paper	7000	9000
American Hunter	J-22-93	Stk & Mig	Paper	7000	9000
American Hunter	J-23-93	Stk & Mig	Paper	7000	9000
American Hunter	J-24-93	Stk & Mig	Paper	7000	9000
American Hunter	J-25-93	Stk & Mig	Paper	7000	9000
Southland Royalty	84-1	Stk & Mig	Paper	7000	8500
Southland Royalty	84-2	Stk & Mig	Paper	7000	8500
Southland Royalty	84-3	Stk & Mig	Paper	7000	8500
Southland Royalty	84-4	Stk & Mig	Paper	7000	8500
Southland Royalty	84-5	Stk & Mig	Paper	7000	8500
Southland Royalty	84-6	Stk & Mig	Paper	7000	8500
Southland Royalty	84-7	Stk & Mig	Paper	7000	8500
Conoco/Meridian	MOICON 8A	Stk & Mig	Dig./Paper	6000	10500
Conoco/Meridian	MOICON 8B	Stk & Mig	Dig./Paper	6000	10500
Conoco/Meridian	MOICON 9A	Stk & Mig	Dig./Paper	6000	10500
Conoco/Meridian	MOICON 9B	Stk & Mig	Dig./Paper	6000	10500
Conoco/Meridian	MOICON 10	Stk & Mig	Dig./Paper	6000	10500
Conoco/Meridian	MOICON 12	Mig	Dig./Paper	6000	10500
Meridian	MOI-NTPRDG-93-1	Stk & Mig	Film/Paper	7000	10000
Meridian	MOI-NTPRDG-93-2	Stk & Mig	Film/Paper	7000	10000
Meridian	MOI-BDHL-92-1	Stk & Mig	Film/Paper	7000	10000
Meridian	MOI-BDHL-92-2	Stk & Mig	Film/Paper	7000	10000
Amoco	GDD-A1	Stk	Film	Sloping	N/A
Amoco	GDD-A2	True Amp	Film	Sloping	9000
Amoco	GDD-AA	True Amp	Film	Sloping	9000
Amoco	GDD-B	Stk	Film	Sloping	N/A
Amoco	GDD-BB	True Amp	Film	Sloping	9000
Amoco	GDD-C	Stk	Film	Sloping	N/A
Amoco	GDD-C	True Amp	Film	Sloping	9000
Amoco	GDD-CC	True Amp	Film	Sloping	9000
Amoco	GDD-D1	Stk	Film	Sloping	N/A
Amoco	GDD-D2	True Amp	Film	Sloping	9000
Amoco	GDD-DD	True Amp	Film	Sloping	9000
Amoco	GDD-EE	Stk	Film	7000	10000
Amoco	GDD-E3	T.A. & Stk	Film	Sloping	9000
Amoco	GDD-K	True Amp	Film	Sloping	9000
Amoco	GDD-L	True Amp	Film	Sloping	9000
Amoco	GDD-M	T.A. & Stk	Film	Sloping	9000
Amoco	GDD-N	Stk	Film	Sloping	N/A
Amoco	GDD-T	Stk	Film	Sloping	N/A
Amoco	GDD-U	True Amp	Film	Sloping	9000
Amoco	GDD-V	True Amp	Film	Sloping	9000
Amoco	GDD-W	True Amp	Film	Sloping	9000
Amoco	GDD-W	Stk & Mig	Film	7000	10000
Amoco	GDD-X	True Amp	Film	Sloping	9000
Amoco	GDD-Y1	Loc Only	N/A	N/A	N/A
Amoco	GDD-Y2	True Amp	Film	Sloping	9000
Amoco	GDD-Z	True Amp	Film	Sloping	9000
Amoco	EE-3	Stk	Film	Variable	8000
Amoco	EE-4	Loc Only	N/A	N/A	N/A
Amoco	EE-5	Stk	Film	Variable	8000
Texaco	19	Rel Amp	Dig./Film	Sloping	7000
Texaco	20	Rel Amp	Dig./Film	Sloping	7000

Texaco	22	Rel Amp	Dig./Film	Sloping	7000
Texaco	21	Rel Amp	Dig./Film	Sloping	7000
Texaco	23	Rel Amp	Dig./Film	Sloping	7000
Texaco	34	Rel Amp	Dig./Film	Sloping	8000
Texaco	35	Rel Amp	Dig./Film	Sloping	9000
Texaco	538	Rel Amp	Dig./Film	Sloping	8000
Texaco	539	Rel Amp	Dig./Film	Sloping	8000
Texaco	540	Rel Amp	Dig./Film	Sloping	8000
Texaco	546	Rel Amp	Dig./Film	Sloping	8000

Stk = Stack Section
Mig = Migrated Section
True Amp = True Amplitude Section
T.A. = True Amplitude Section
Rel Amp = Relative True Amplitude Section
Dig = Digital Data Available

which produces generally higher resolution data provided that it has a small sampling interval and has not been filtered too tightly. Figure 2 is an example of the Southland Royalty data from line 84-2. These data where acquired using four vibrators sweeping twelve times from 14 to 80 hertz with a recording sample interval of 2 milliseconds. This produced good quality data that looks better than the 6 fold data but not as clean as the 40 fold data shown in figure 1.

Almost all of the data were processed conventionally through final Common Depth Point (CDP) stack and migration. However, most of the data from Amoco were processed using a sequence that produced true relative amplitude stacked sections with no Automatic Gain Control (AGC) applied. Figure 3 is an example of a true relative amplitude processed section from the Amoco survey. Note that the data looks "washed out" with few good high amplitude reflections. The project did not have digital data from the Amoco survey and could not reprocess the data to make it look similar to the other surveys on the reservation. The lack of good reflections made this data extremely hard to interpret. We were fortunate to have better quality lines from the Conoco/Meridin and Texaco oil companies in the same area as the true amplitude processed Amoco data.

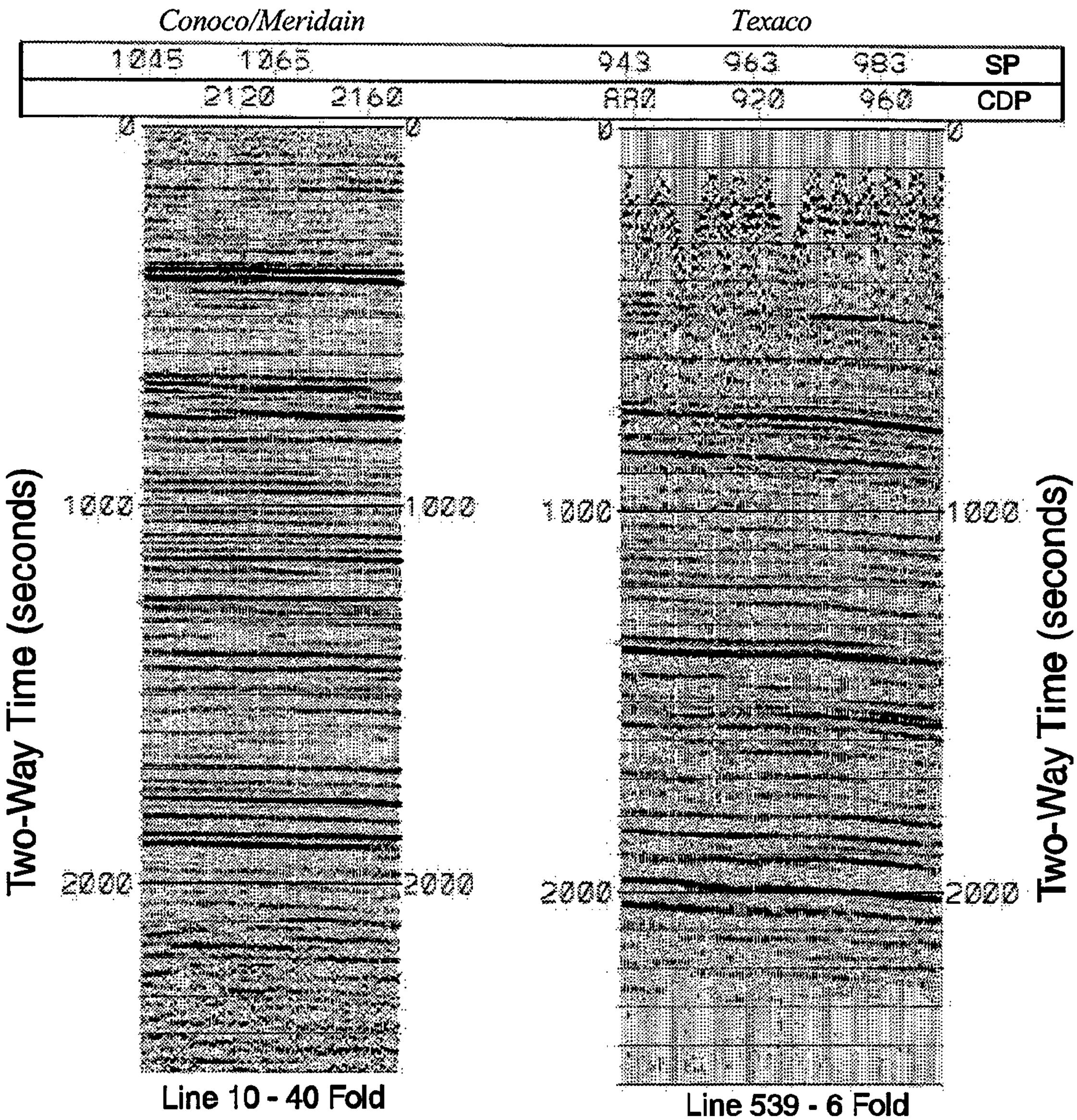

Figure 1. Comparison of reprocessed 4000% (40 fold) multichannel seismic reflection data from Conoco/Meridian oil companies with 600% (6 fold) multichannel seismic reflection data from Texaco. Note the improved signal to noise ratio and resolution in the 40 fold data on the left versus the 6 fold data on the right.

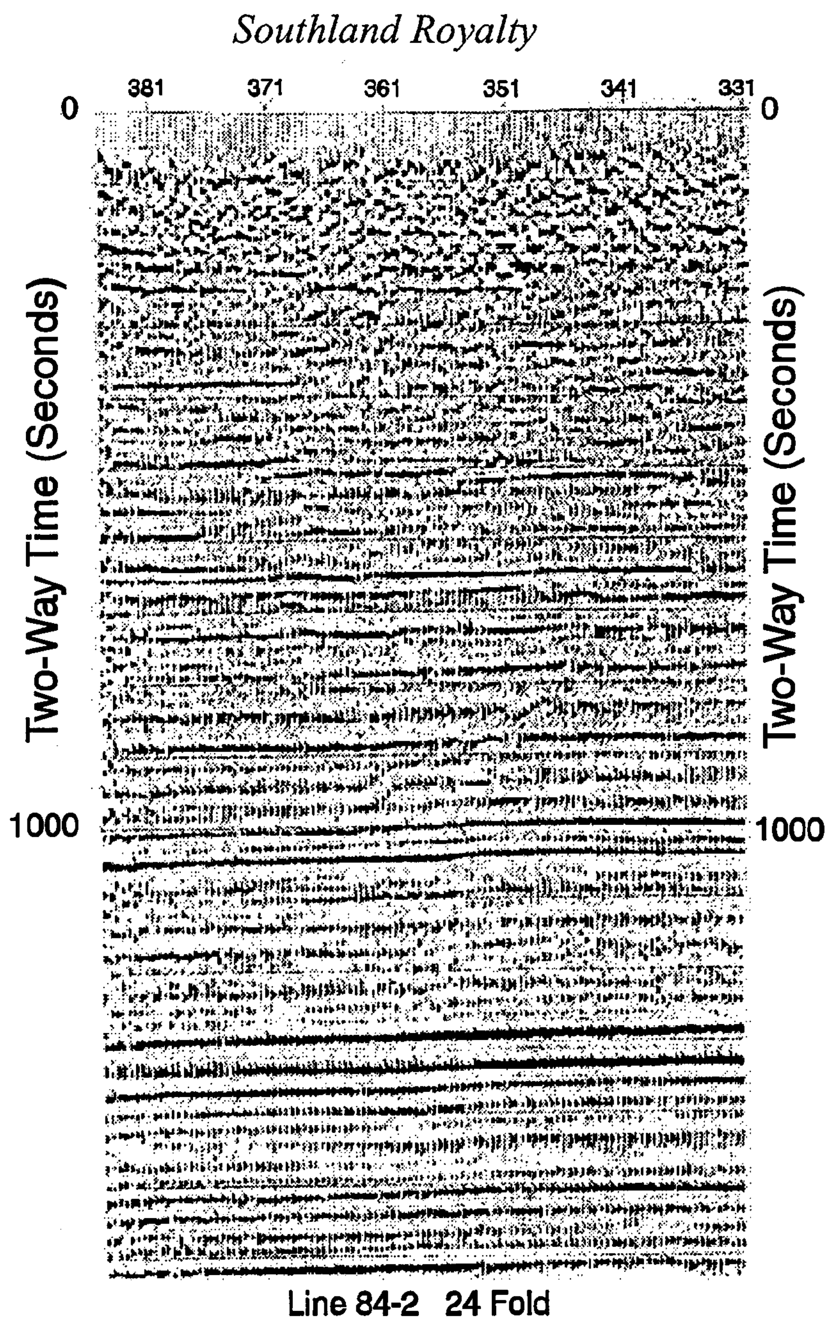

Figure 2. Portion of Southland Royalty line 84-2 which was acquired using a vibrator source rather than a dynamite source. Data is 2400% (24 fold) and recorded at a 2 millisecond sample interval.

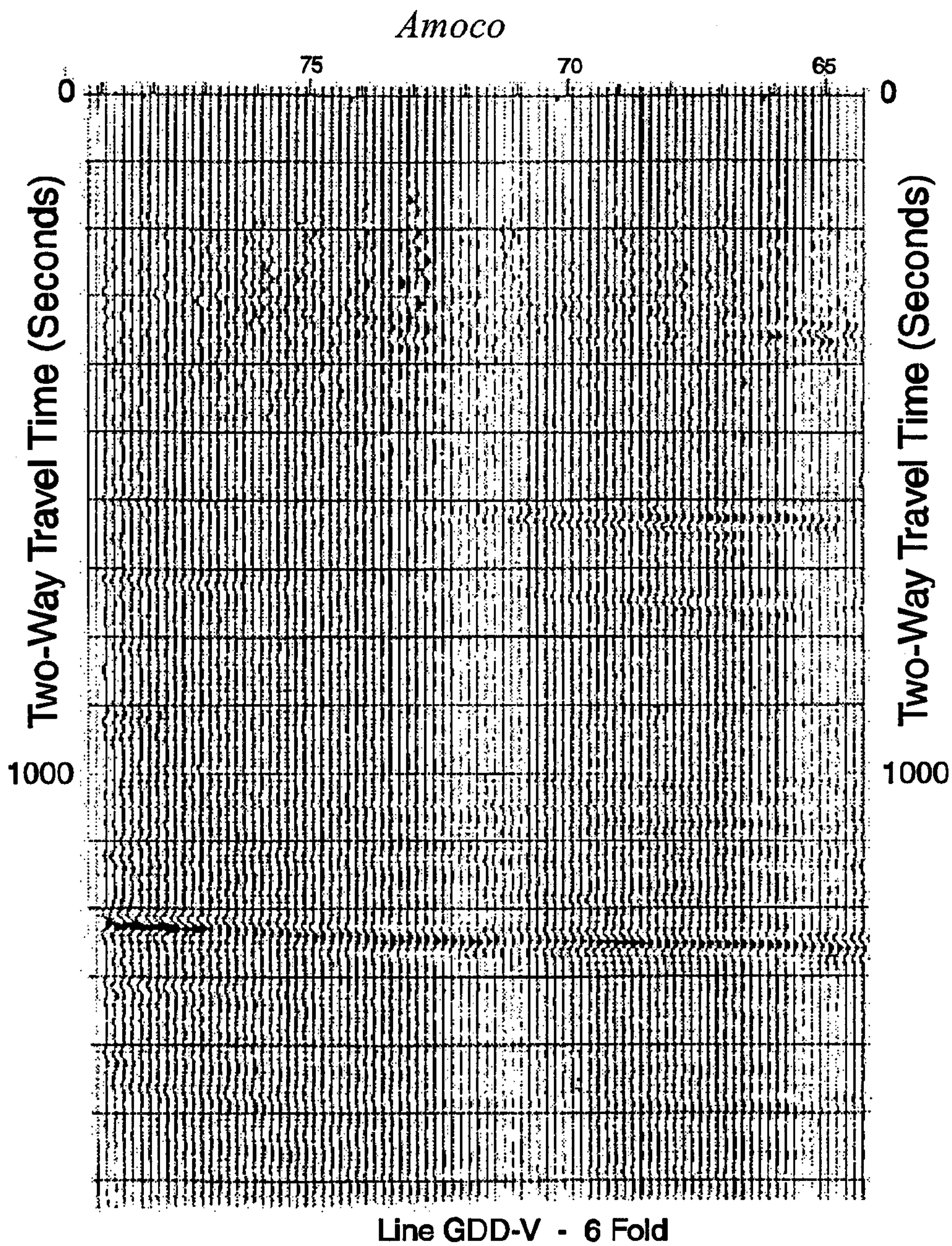

Figure 3. Portion of Amoco seismic line GDD-V which used True Relative Amplitude processing rather than normal automatic gain control (AGC) to balance trace amplitudes. Note the absence of good strong reflections which makes this section difficult to interpret structurally.

Seismic Data Reprocessing

The project was able to acquire digital data for some of the American Hunter, Conoco/Meridian, and Texaco seismic surveys only (See table 2).

The American Hunter survey came predominantly as paper sections but a magnetic tape with processed versions for four of the lines in SEG-Y format accompanied the hardcopy. These lines were loaded onto a Landmark Graphics ProMAX seismic data processing system and displayed to confirm that the tape could be read and that both the stacked and migrated data were on the tape. Since unprocessed data or the acquisition logs were not available it was not possible to reprocess these four lines. In order to match other data used in the interpretation a bandpass filter of 20-28-80-100 hertz was applied along with an automatic gain control (AGC) with a sliding scale window of 500 milliseconds which balanced the trace amplitudes from the top to the bottom of the section. The data were then re-displayed at horizontal and vertical scales that matched the hardcopy format seismic data.

The Texaco survey also came in both digital and hardcopy form. For this survey two 8mm magnetic tapes were supplied, one with the unprocessed field data and the other with the processed stacked data. The observer's reports and the surveyor's notes came along with the tapes so reprocessing from the field data could be performed. The processed stack data were loaded onto the ProMAX system for re-display at a scale matching other lines used in the interpretation. No reprocessing was performed on this data due to time constraints. The trace headers were modified to contain the shotpoint number and an AGC with a 500 millisecond sliding window and was applied before re-display. Data on the tape containing the processed data were found to match the hardcopy and no further reprocessing was performed on this data set.

The digital data for the Conoco/Meridin survey consisted of unprocessed field data only. Support data were available for lines 8, 9, and part of 10. No support data were available for line 12. Since no digital processed data were available it was decided to reprocess lines 8, 9 and part of 10 to confirm the processing used to generate the hardcopy sections and to provide the Tribe with processed digital data for future loading onto an interpretation workstation.

Originally lines 8 and 9 of the Conoco/Meridian seismic survey were acquired as single lines that spanned areas both on and off the reservation. When the data were supplied to the Tribe, and later to the BIA, Conoco/Mewridain displayed only those portions of the data on Indian lands. Likewise when the digital data were released to the Tribe and the BIA only those portions of the digital line data overlying reservation lands were put on tape. This meant that it was necessary to reprocess lines 8 and 9 in segments. Line 8 then became lines 8A and 8B, and line 9 became lines 9A and 9B. Only the southern portion of line 10 was located on Indian lands so that is the only part of the line present in digital form.

Identical steps were used in the processing of lines 8A, 8B, 9A, 9B, and 10. This assured that all of the lines would have a consistent appearance making it easier to correlate between lines. The processing sequence is shown in figure 4. The steps illustrated in figure 4 represent those typically used in the petroleum industry to process land based seismic data. EPIC Geophysical processed the data for Conoco/Meridian originally and used all of the same steps with the addition of pre-stack refraction statics, pre-stack trim statics, post-stack phase shift migration, and post stack FX deconvolution. They did not perform a zero-phase spiking deconvolution prior to their residual statics or a wavelet processing step after CMP stack.

Figure 5 shows a typical shot record after geometry definition and application. This record shows a good signal to noise ratio where the hyperbolic primary reflections are easily seen. The steeply dipping events cutting across the primary reflections are a result of ground roll motion from the shot being recorded along the receiver line. Subsequent processing steps such as filtering and stacking tend to diminish these events and enhance the primary events. Noisy traces such as the one at channel 65 were zeroed and the noise preceding the first breaks was muted in the trace edit processing step. Figure 6 shows the same shot record after trace edit and mute, zero-phase spiking deconvolution and single window zero-phase bandpass filter. Notice how well the effects of ground roll have been removed by the application of the bandpass filter. Notice also that the primary wavelets have been compressed and the resolution of the primary events have been enhanced by the application of zero-phase spiking deconvolution and zero-phase bandpass

Conoco/Meridian Seismic Data Processing Sequence

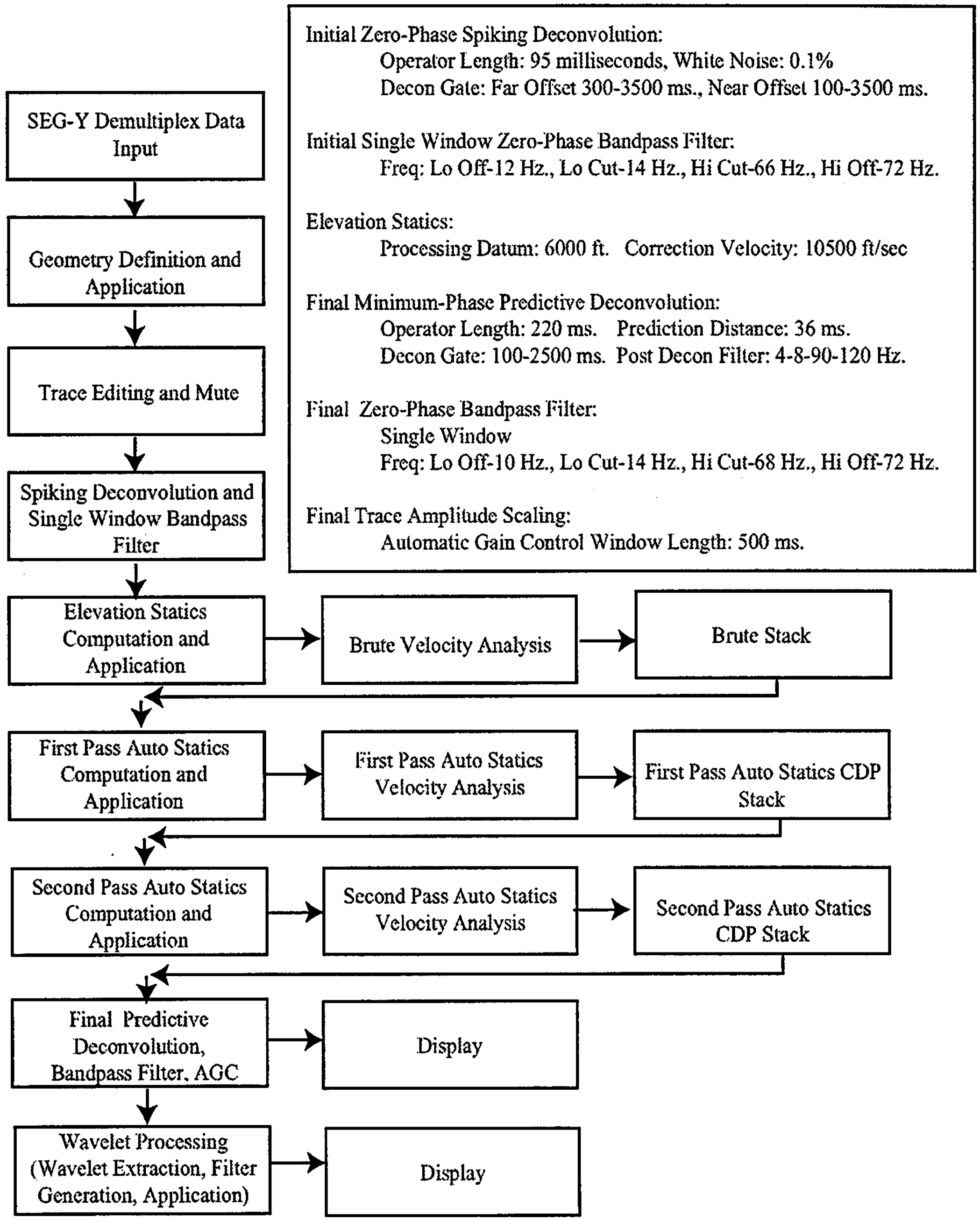

Figure 4. Diagram showing the sequence used to reprocess the Conoco/Meridian seismic data. This sequence was used for Conoco/Meridian seismic lines 8A, 8B, 9A, 9B, and 10.

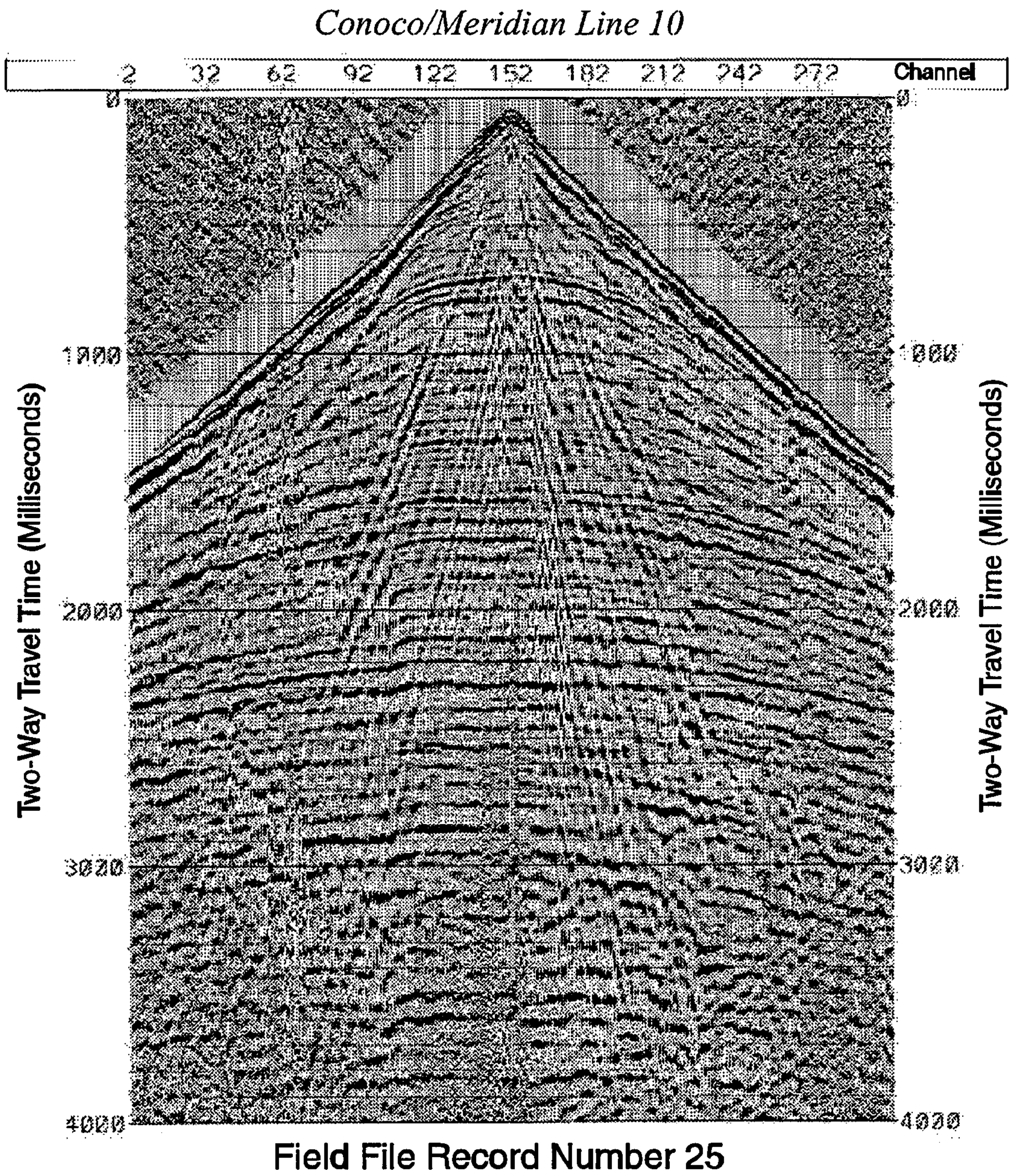

Figure 5. Example of demultiplexed field record with geometry definitions in the header from Conoco/Meridain line 10. Steeply dipping events represent ground roll energy coming from the shot through the receiver line.

filter steps. After the spiking deconvolution and bandpass filter steps the records are ready for an initial velocity analysis and CMP stacking. From figure 6 notice in the circled area the effects of statics problems caused by the difference in receiver and shot elevations. These will be resolved by using multiple passes of the data through residual auto statics routines. Figure 7 is the same shot record after a second pass through residual statics determination and application. Notice how the small time differences between traces as shown in figure 6 have been removed resulting in smoother looking primary event hyperbolas. These records are now ready for final CMP sort, velocity analysis, and stack.

Figure 8 shows a portion of line 10 after the shot records have been processed through zero-phase spiking deconvolution, zero-phase bandpass filter, velocity analysis, and CMP stack. No residual statics have been applied to the records prior to the CMP stack shown in this figure. Note the loss of resolution for two high amplitude reflections at points A and B on figure 8. Figure 9 is the same portion of line 10 after the applications of two passes through residual statics and final minimum-phase prediction deconvolution and single window zero-phase bandpass filter. The overall appearance of the section is less noisy with the same events labeled A and B being more coherent and therefore easier to interpret. Application of post-stack wavelet processing has made only a very subtle change in the overall appearance of the data as noted by comparing the final stack section of figure 9 with the same portion of data after wavelet processing shown in figure 10. Since the data shows little structural complexity, post-stack time migration was not applied to the Conoco/Meridian reprocessed data.

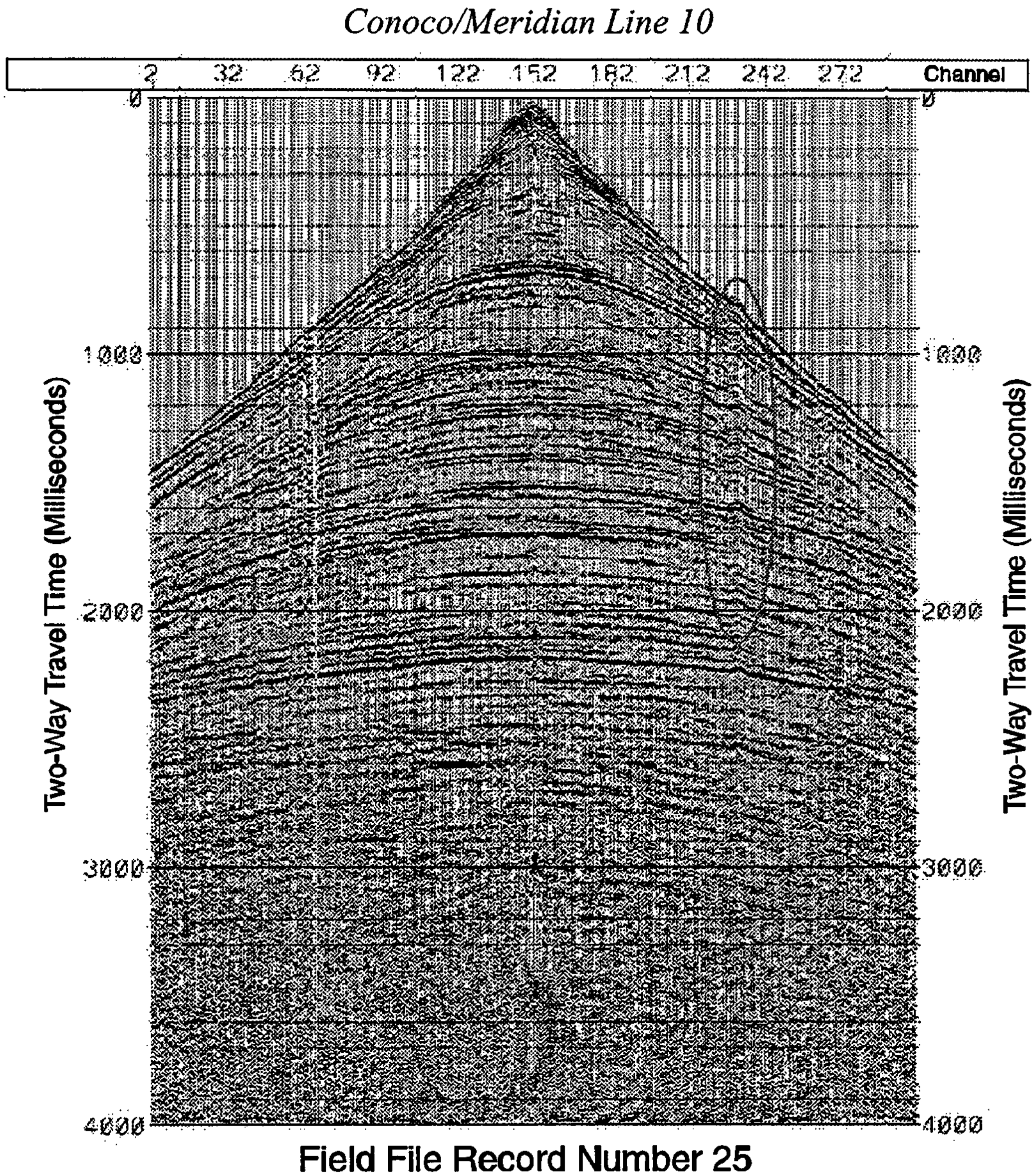

Figure 6. Example of the same demultiplexed field record shown in figure 5 from Conoco/Meridain line 10 with trace editing, top mute, zero-phase spiking deconvolution, and single window zero-phase bandpass filter applied . Note how filtering has removed almost all of the effects of ground roll from this record. The area circled shows static problem caused by the difference in shot and receiver elevations.

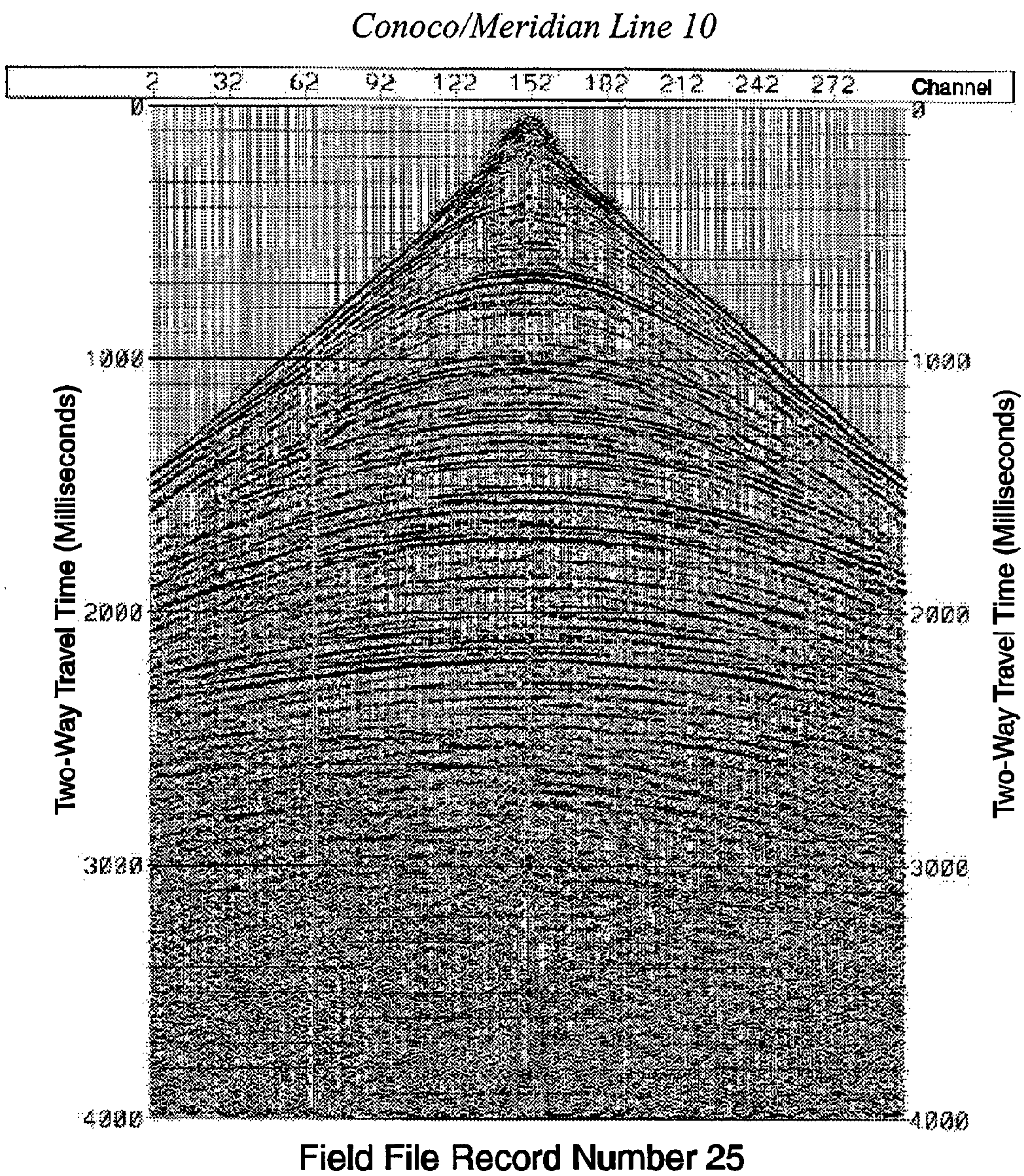

Figure 7. Example of of the same field record shown in figure 6 from Conoco/Meridain line 10 after elevation statics and two passed of residual automatic statics have been applied. The static problem circled in figure 6 has now been resolved and other small time shifts in the primary reflection hyperbola have been removed resulting in significantly more coherent reflections.

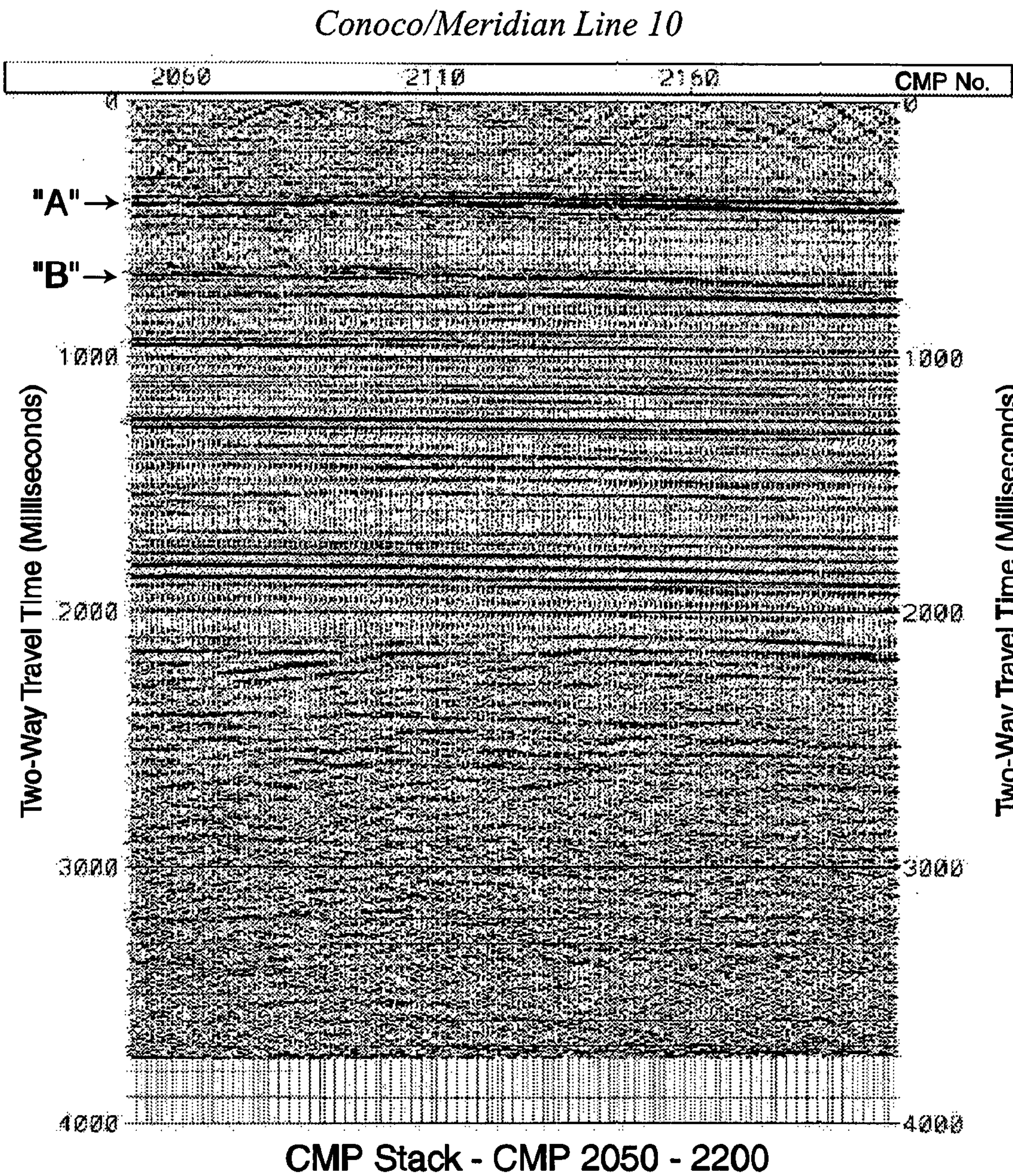

Figure 8. Portion of Conoco/Meridian line 10 after shot records have been passed through trace editing, top mute, zero-phase spiking deconvolution, single window zero-phase bandpass filter, elevation statics corrections, velocity analysis, and CMP stack. No residual automatic statics have been applied. Note poor reflection coherency at points "A" and "B", especially between CMP 2050 and 2100.

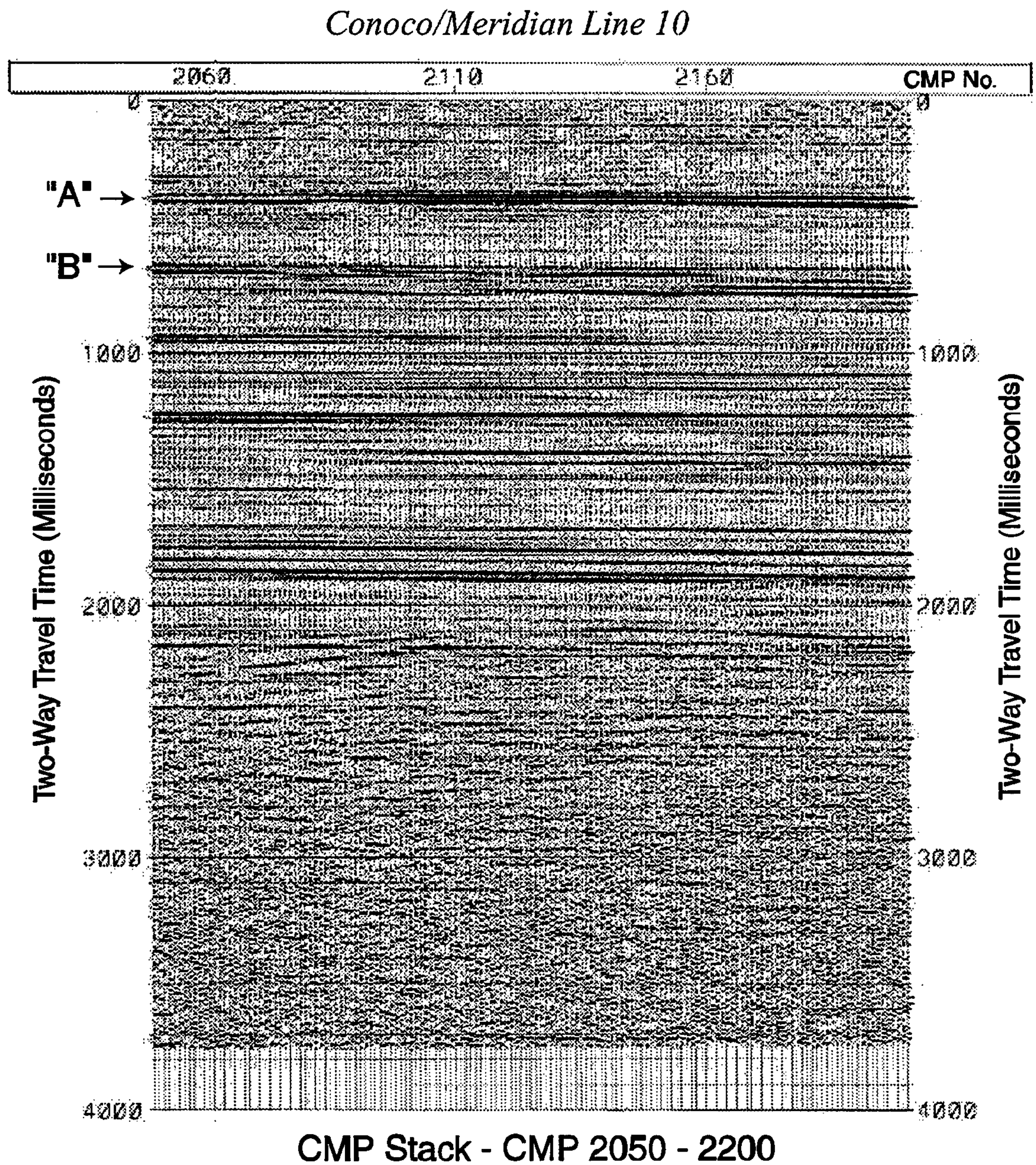

Figure 9. Same portion of Conoco/Meridian line 10 as shown in figure 8 after shot records have been passed through two passes of residual automatic statics computation and application before velocity analysis, and CMP stack. Note how the reflection coherency at points "A" and "B" between CMP 2050 and 2100 has been improved by the resolution of statics problems.

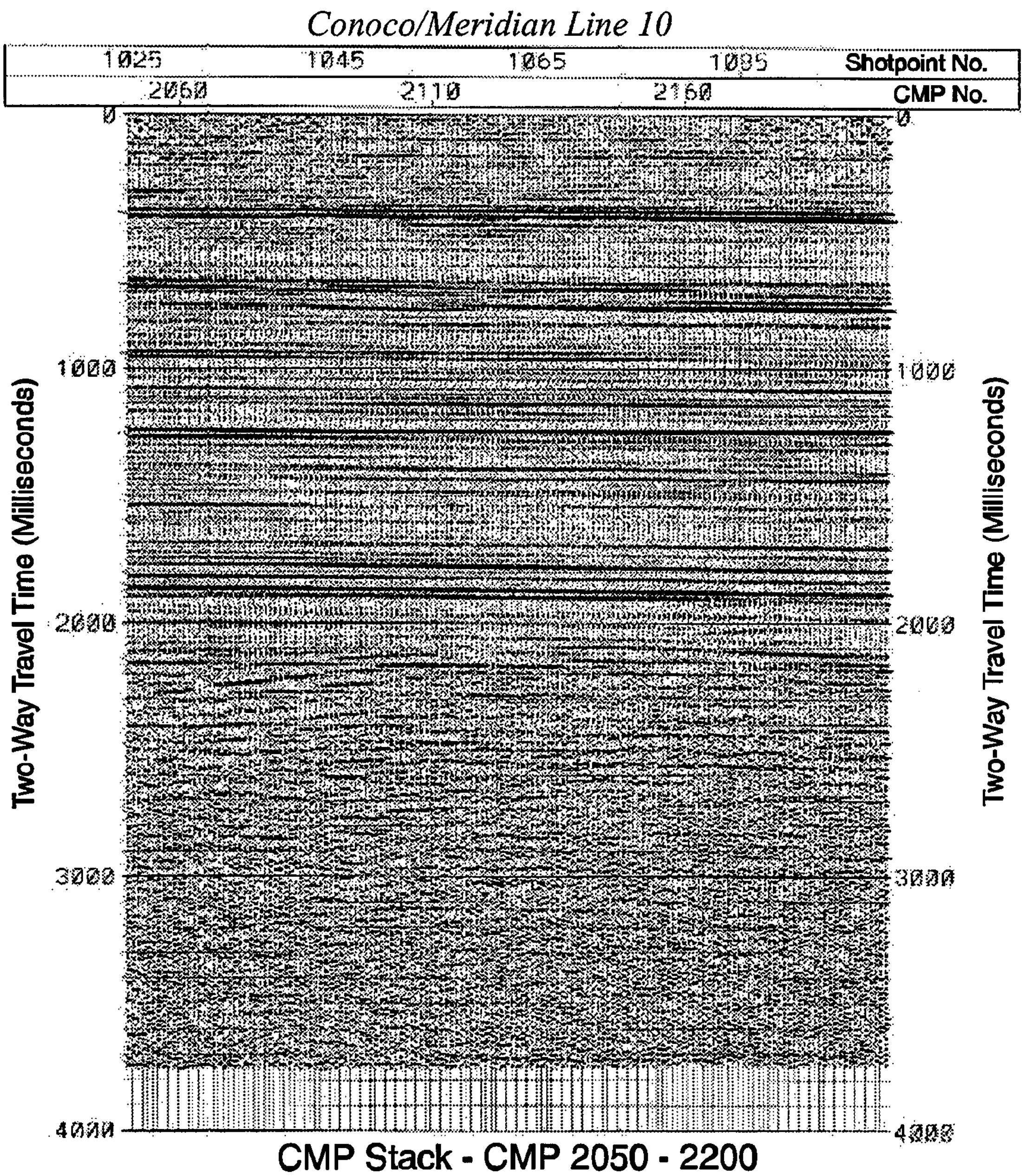

Figure 10. Same portion of Conoco/Meridian line 10 as shown in figure 9 after wavelet processing the final stacked section.

Comparing the originally processed data with the reprocessed data shows that the reprocessed data looks as good as the original processed data with all of the same major reflections present. In figure 11 one can see that the original processing yields slightly better results in the section above 300 milliseconds as a result of the application of refraction statics and the overall original processing looks less noisy as a result of the post-stack FX deconvolution step. Still, the reprocessing is extremely interpretable, especially in a structural sense. Reprocessing the selected Conoco/Meridain data did fulfill its purpose of confirming the original processing and producing good quality processed data in digital form for future use by the Jicarilla Apache Tribe or the BIA on an interpretation workstation.

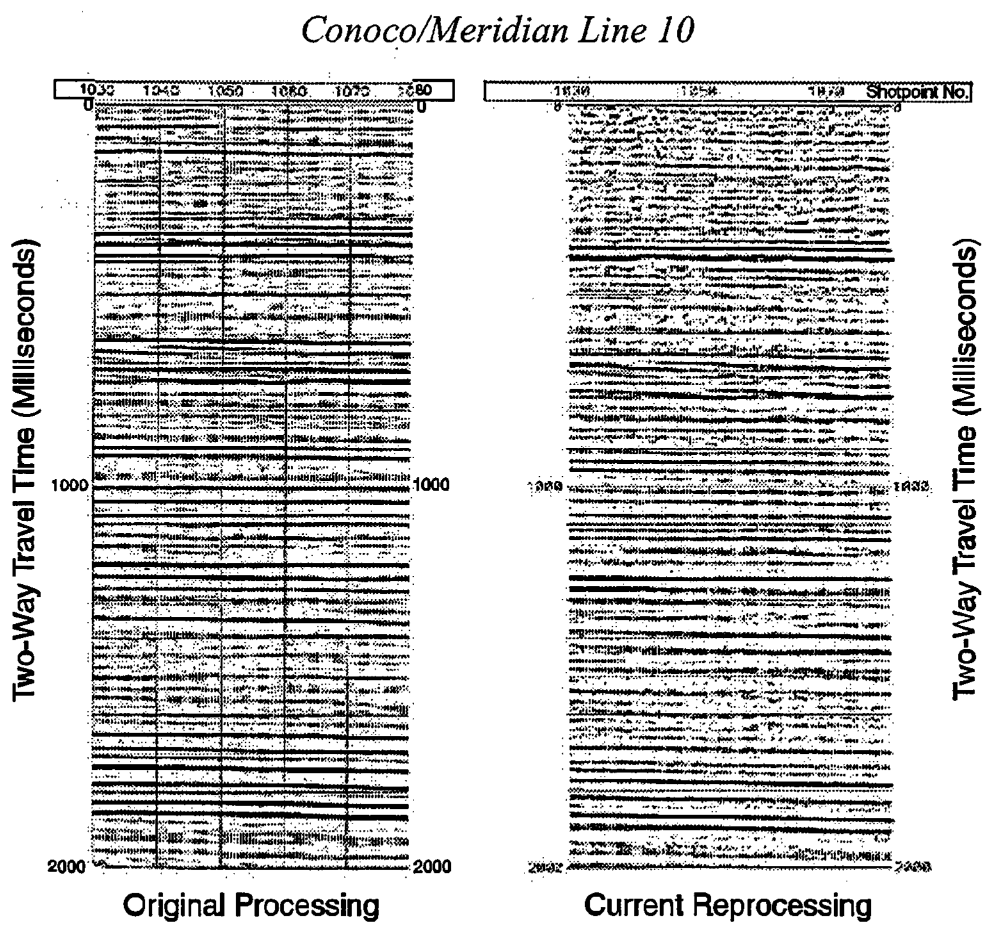

Figure 11. Comparison of identical portions of the final original processing and the final current reprocessing for Conoco/Meridian line 10. Post stack phase shift migration and FX deconvolution has been applied to the original processing on the left whereas the current processing on the right has had only wavelet processing applied post stack.

Synthetic Seismogram Correlation

It is impossible to complete an interpretation of the seismic data without knowing which reflections on the seismic data correlate to known geologic boundaries. Geologic formation tops, lithology, density, and acoustic properties are usually determined from drill cuttings, drill cores, and petrophysical logs retrieved from oil and gas wells. An accepted way to match geologic information gathered in well with adjacent surface seismic reflection data is to generate an artificial seismic section called a synthetic seismogram from the petrophysical logs commonly run in the oil and gas wells.

A one-dimensional synthetic seismogram is produced by convolving a seismic wavelet with a reflectivity function (Sheriff, 1989). The wavelet is sometimes an assumed wavelet such as a Ricker or Orsby bandpass wavelet or a wavelet that has been extracted from the actual surface seismic data. The reflectivity function sometimes involves primary reflections only, primary and specific multiple reflections, or primary and all multiple reflections. The reflectivity function is usually that calculated for normal incidence from velocity data primarily but can include density data, if it is known and is reliable. For this study all synthetic seismograms where generated using the velocity data only. When no density data are available the software holds the density value at a constant value of 1, therefore the density contribution has no effect on the result. All synthetic seismograms where produced using the 1-D synthetic seismogram software from DigiRule, Inc. of Calgary, Alberta in Canada.

Plate 1 shows the location of the surface seismic reflection data and the location for selected wells that were used in this study. For a well to be most useful it must have at least a borehole sonic log and penetrate most of the sedimentary section. Most of the wells on the reservation that are adjacent to the surface seismic data had only electrical logs run in them or were exceptionally shallow. These factors limited the number of wells to only 6 where synthetic seismograms could be produced that would be close enough to the seismic data and deep enough to be reliable. The borehole sonic logs for these wells were digitized using software and hardware from DigiRule and the results used in their 1-D synthetic seismogram generation software.

The reflectivity function is a time function or time series representing reflecting interfaces from geologic boundaries and the reflection coefficients that they produce (Sheriff, 1989). The reflection coefficient for normal incidence between an interface, or geologic boundary, separating material of different densities and velocities is:

$$R = (\rho_2 V_2 - \rho_1 V_1) / (\rho_2 V_2 + \rho_1 V_1)$$

ρ_1 = Density for material 1

ρ_2 = Density for material 2

V_1 = Velocity for material 1

V_2 = Velocity for material 2

The reflectivity function is usually presented as a "stickgram" because the reflection coefficient produces a spike at each sampled interface. The reflection coefficient time series is then convolved with a wavelet to produce the synthetic seismogram. All of the wavelets used in this study were zero-phase Ormsby bandpass wavelets whose frequencies varied to produce the best match with the surface seismic data.

There were several wells in key locations where synthetic seismograms were generated and correlated with nearly adjacent surface seismic data. Three wells in particular were located in the northern, middle, and southern sections of the reservation. These wells all had good borehole sonic logs and were either deep, penetrating the entire sedimentary section, or penetrated at least the Cretaceous section and where close to a seismic line. The three key wells are:

Pan American Petroleum Corporation

Pagosa Jicarilla No. 1

23 - 32N - 3W

Rio Ariba Co., New Mexico

TD – 3,215 meters (11,549 ft.)

Sunray DX

Jicarilla Tribal No. 1

34 - 30N - 3W

Rio Ariba Co., New Mexico

TD – 2,530 meters (8,300 ft.)

Pan American Petroleum Corporation

Jicarilla Tribal 72 No. 1

6 - 23N - 3W

Rio Ariba Co., New Mexico

TD – 4,115 meters (13,500 ft.)

Figure 12 shows the synthetic seismogram produced from the borehole sonic log for the Pan American Petroleum Pagosa- Jicarilla No. 1 well along with the gamma ray and short normal resistivity curves and the reflection coefficient "stickgram". Formation tops for key interfaces within the sedimentary section as picked from the geophysical logs are included. The software calculates a time to depth relationship from the velocity log so that formation tops entered in depth can be converted to time. This well is located approximately 305 meters (1000 feet) northwest of shotpoint number 1275 on Amoco Production Company seismic line EE-3.

Using the normal polarity synthetic seismogram generated from the Pagosa-Jicarilla No. 1 well a match was attempted with Amoco Production Company seismic line EE-3 at shotpoint 1275 (figure 13). Unfortunately, the 6-fold seismic data are very poor in the area of the correlation. This is most likely due to the fact that shotpoint 1275 falls at the end of the line where fold is dropping off and the seismic line in this area is imaging a large structure in the subsurface where most energy is not being reflected to the full receiver line laid out at the surface. However, fair correlations can be made, especially at the base of the Mesaverde /

top of the Point Lookout, Greenhorn / Dakota, and Morrison / Entrada formation boundaries. Good reflections at roughly 1.72 seconds on the seismic data

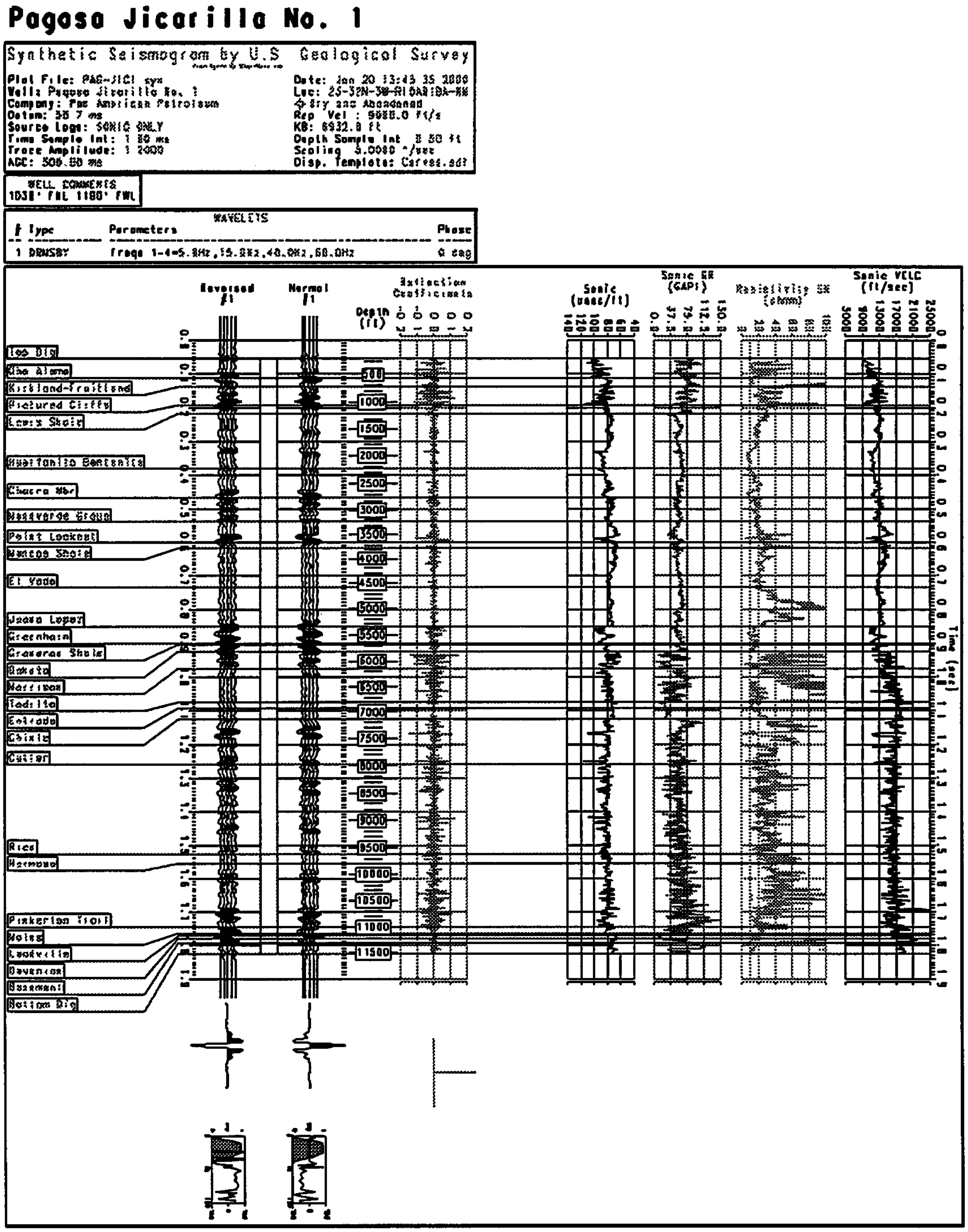

Figure 12. Synthetic seismogram generated from the borehole compensated sonic and formation density logs for the Pan American Petroleum Pagosa-Jicarilla No. 1 well located in section 23 of township 32 north and 3 west. This well is adjacent to the end of Amoco seismic line EE-3 located in the far northwestern part of the Jicarilla Apache Indian Reservation as shown in Plate 1.

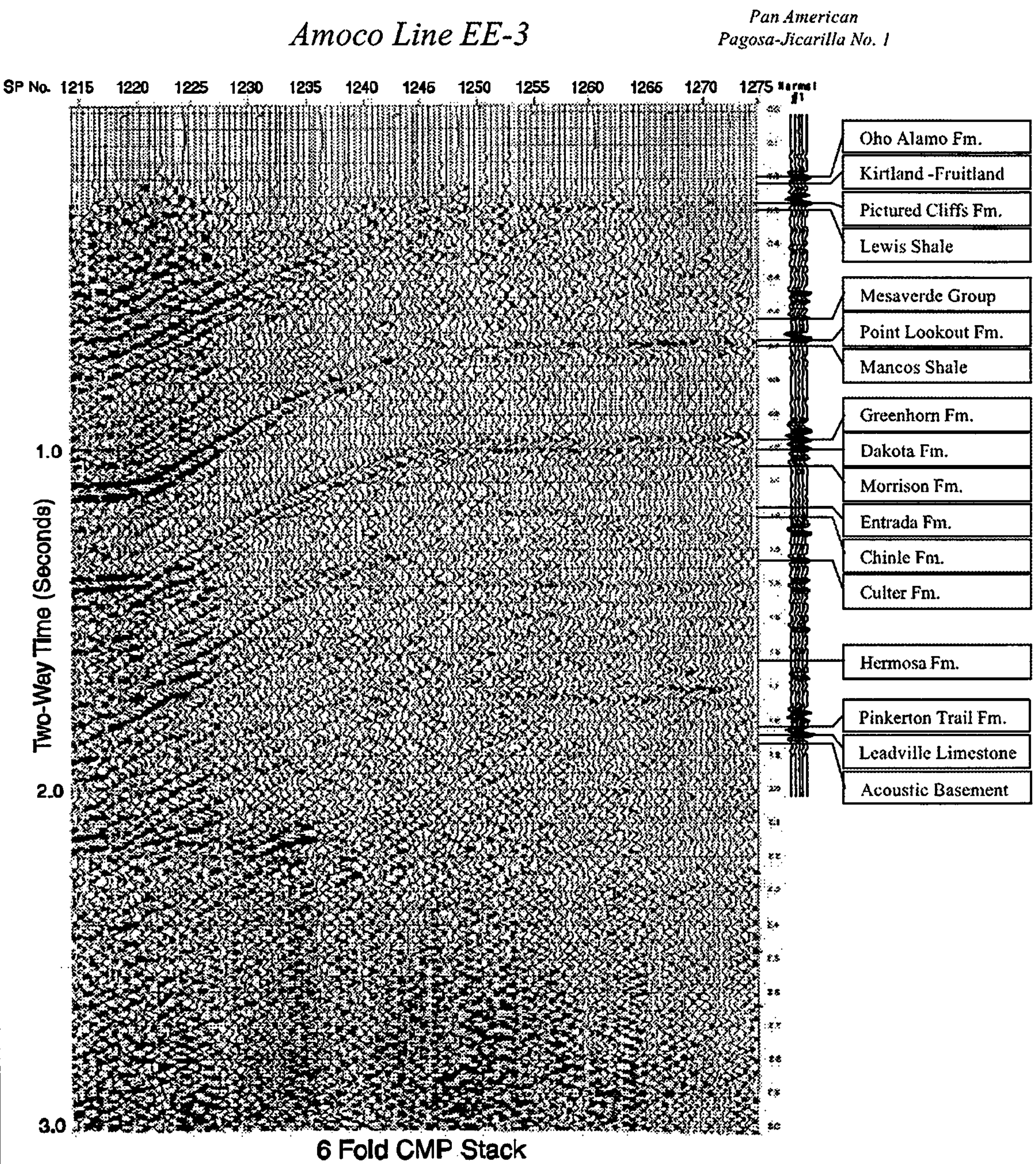

Figure 13. Portion of Amoco seismic line EE-3 located in the northwestern part of the Jicarilla Apache Indian Reservation showing the synthetic seismogram tie with the Pan American Petroleum Corp. Pagosa Jicarilla No. 1 well located approximately 1000 feet north of shotpoint 1275. Geologic horizons from figure 13 have been included to show the corelation between reflections on the synthetic seismogram with those on the seismic data.

may be from uplifted basement rocks which do not correlate well with the basement pick from the well at about 1.85 seconds on the synthetic seismogram.

The Southland Royalty seismic data, which lies further south, offers a much better correlation with the synthetic seismogram from Jicarilla Tribal No. 1 well. Figure 14 shows a good tie between the well data and the actual seismic data. The well is located approximately 457 meters (1500 feet) south of seismic line 84-6 at shotpoint 181. This is a relatively shallow well with a total depth of 2,530 m (8,300 feet) and only penetrated Cretaceous Mesaverde rocks. However, there are very good correlations at the Oho Alamo, Kirtland/Fruitland, and Mesaverde interfaces. The higher fold seismic data produces a much better tie with the synthetic seismogram produced from the borehole sonic log. The short normal resistivity curve has been plotted next to the synthetic seismogram to help illustrate the location of geologic interfaces.

The last well used in this phase of the study was the Pan American Petroleum Jicarilla Tribal 72 No. 1 well located in the southern part of the reservation. The well is located less than 150 meters (500 feet) from Amoco Production Company seismic line EE-5 at shotpoint 1236. This is a deep well penetrating the entire sedimentary sequence from Tertiary to acoustic basement. The gamma ray, short normal resistivity, and the spontaneous potential log curves are displayed along with the sonic and velocity curves for this well on figure 15. Detailed formation tops are also shown as picked from the well logs. The formation tops picked from the logs in depth have been plotted in time according to a time to depth function calculated from the borehole sonic log as before. Good reflections on

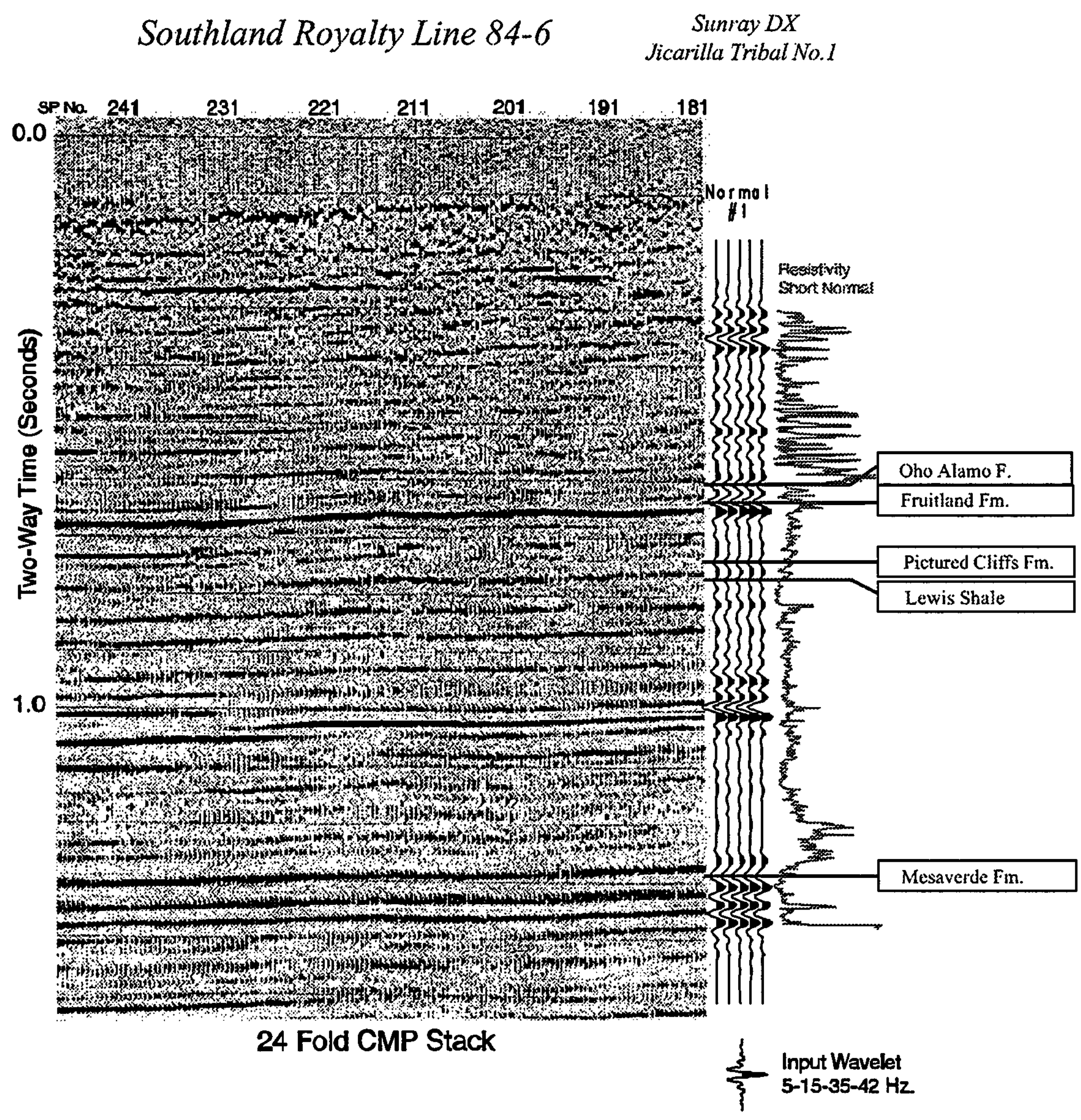

Figure 14. Portion of Southland Royalty seismic line 84-6 located in the west central part of the Jicarilla Apache Indian Reservation showing the synthetic seismogram tie with the Sunray DX Jicarilla Tribal No. 1 well located approximately 1500 feet south of shotpoint 179. The geologic horizons picked from the short normal resistivity curve are shown along with the synthetic seismogram.

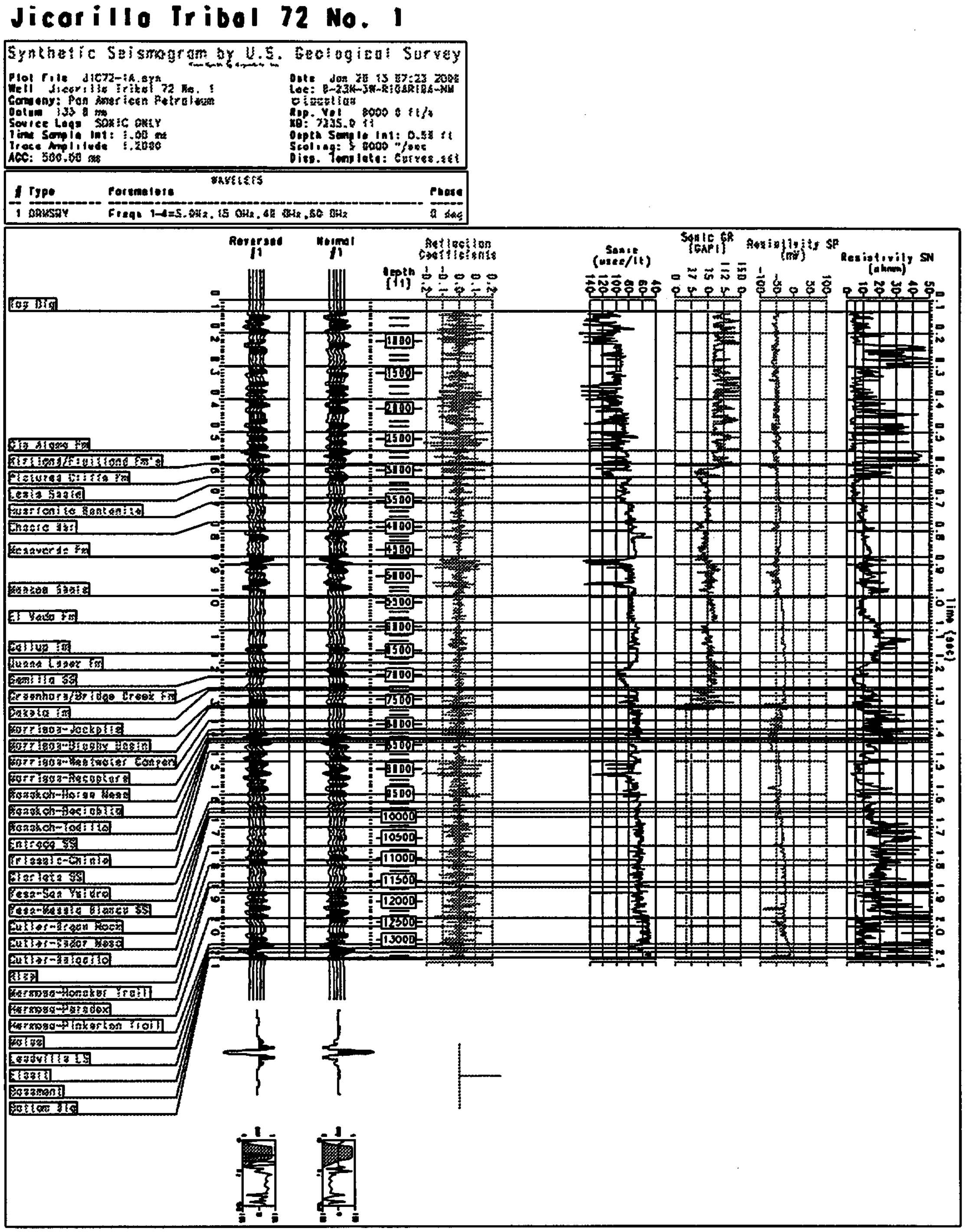

Figure 15. Synthetic seismogram generated from the borehole compenstated sonic log for the Pan American Petroleum Company Jicarilla Tribal 72 No. 1 well located in section 6 of township 23 north and range 3 west. This well is adjacent to Amoco seismic lines EE-5 and GDD-L shown on Plate 1.

the synthetic seismogram appear at the top of the Oho Alamo, Pictured Cliffs, Mesaverde, Dakota, Entrada, Leadville, and basement interfaces. As with the Pagosa-Jicarilla No. 1 well the Jicarilla Tribal 72 No. 1 well ties to 6-fold data which is not as good as the 24-fold or greater data of either the Southland Royalty, American Hunter, or Conoco/Meridian data. However, there seems to be a good match at several interfaces. Figure 16 shows that there is a good seismic to synthetic tie at the Oho Alamo, Pictured Cliffs, Lewis Shale, Dakota, Entrada, and basement levels. Other interfaces, especially the Mesaverde, Mancos Shale, and Cutler correlate to sections of the seismic data that are extremely noisy. It is difficult to determine if reprocessing this older 6-fold data would produce a seismic section that is easier to correlate to the synthetic data.

Two wells in the vicinity of the American Hunter seismic survey had sonic logs available but these were highly deviated holes that bottomed in Cretaceous Mancos Shale. The deviation survey information was not available to the project so the logs could not be converted to true vertical depth and thus could not be used to make relevant correlations. No other wells with good sonic log information where located near enough to available surface seismic data to make reliable correlations. Project personnel determined that the correlations that were made using the three key wells provided enough information to perform a structural interpretation from grid of seismic lines

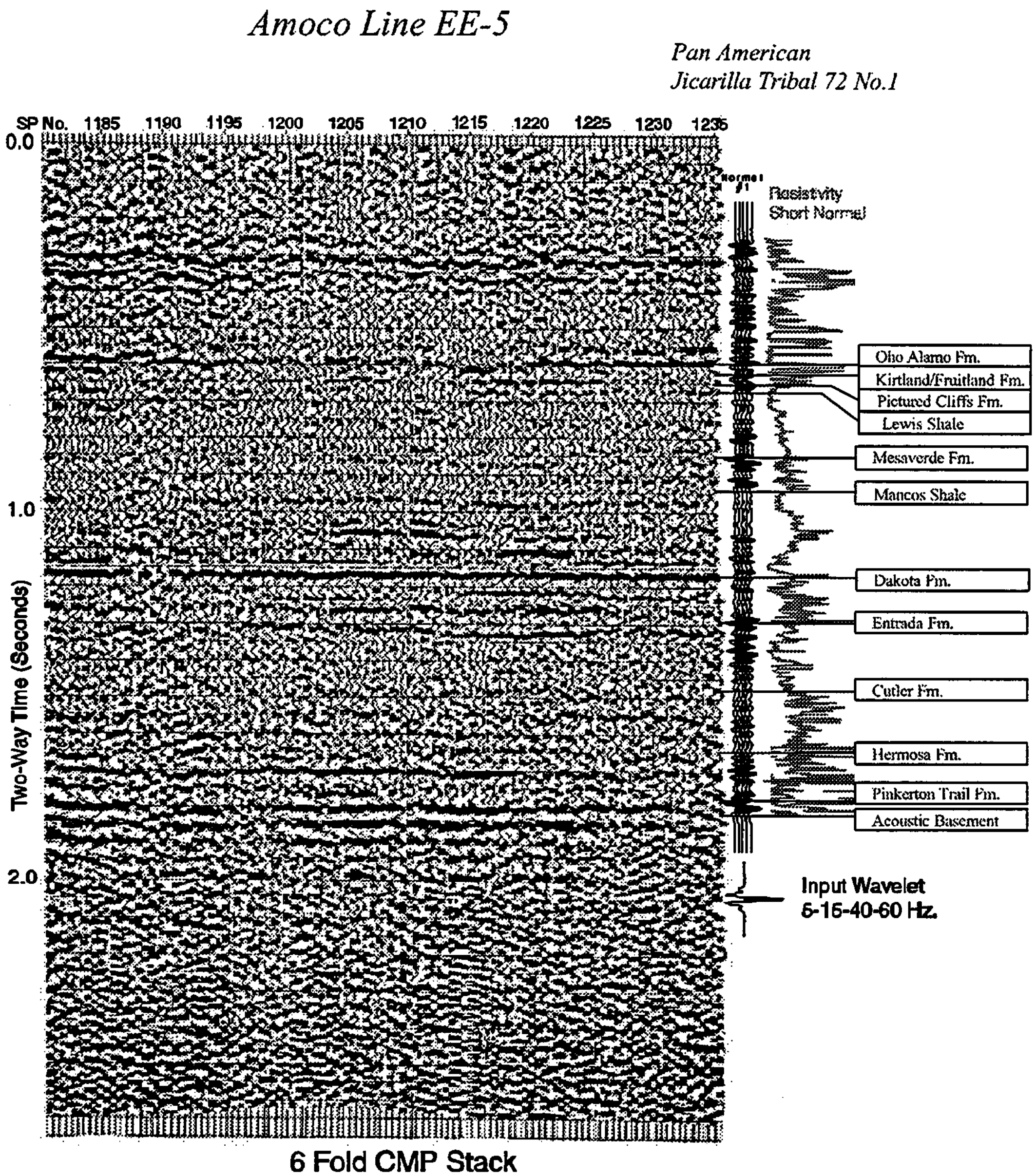

Figure 16. Portion of Amoco seismic line EE-5 located in the south central portion of the Jicarilla Apache Indian Reservation showing the synthetic seismogram tie with the Pan American Petroleum Jicarilla Tribal 72 No. 1 well located directly at shotpoint 1236. Geologic horizons along with the short normal resistivity curve are shown together with the synthetic seismogram.

Structural Analysis

Interpretation of the 2-D reflection seismic data provided for the Jicarilla Apache Reservation was severely limited by several factors: 1. The quality of data was highly variable, particularly since only paper prints were available for many of the lines; 2. The lines were shot, processed, and displayed using different parameters including different datum planes (a number of which are sloping); 3. Little well control is available below the Cretaceous part of the section; and 4. Only those parts of the lines within the Reservation were available. These limitations confined our regional interpretations to analyses of the faulting at the basement, Mesaverde, and Pictured Cliffs horizons. In most cases, we have also confined ourselves to mapping straight-line fault segments since the data are not normally spaced closely enough together or the faults distinctive enough to justify drawing curved lines. Consequently, the resulting maps should be considered first approximations at best.

In general, the patterns of faulting in the higher parts of the section (plates 2 and 3) reflect the basement pattern (plate 4) even though very few of the faults can be shown to extend continuously from the basement through the entire section. In all cases though, demonstrable offset at the mapped horizon was required in order to interpret a fault. Because of the multiple periods of movement on many of the faults, this requirement also insures that the maps will be first approximations only. Based on fault strikes and density, three structural provinces are identified within the general area of the Jicarilla

Reservation. These will be discussed separately and identified simply as the southern, northwestern, and northeastern areas.

Southern Area

The southern area includes all of the southern part of the Reservation, T22N-T26N. Seismic data in this area is the most difficult to deal with because there are so many different sources and types of data. Throughout most of the area, the interpreted fault pattern generally corresponds with that identified through much of the San Juan Basin by Taylor and Huffman (1998), that is, a predominantly orthogonal pattern of N55^{o}-70^{o}W and N30^{o}-45^{o}E fault trends at the top of basement (Plate 4) inherited from the Precambrian and reactivated at various times throughout the Phanerozoic. Although similar, trends in the Mesaverde (Plate 3) and Pictured Cliffs (Plate 2) tend to be more northerly and easterly. Several deviations from this pattern are worth noting, however.

Interpreted along the southeastern edge of the study area were several north-south and east-west faults at all three horizons. The same directions have been mapped in other places in the San Juan Basin and are also thought to be inherited from the Precambrian. We believe the dominance of this direction along the eastern side of the southern area and in the eastern area is related to the NS-trending Nacimiento Fault and Rio Grande Rift.

An irregularly shaped structural high involving the entire sedimentary section occurs along the southern boundary of the Reservation from R3W to R5W including nearly all of T22N, R4W and extending into the southwestern corner of T23N, R4W (Plates 2 and 3). The eastern and western margins of the high are underlain by northeast trending basement thrust faults with opposing vergence but we could not determine if these faults (Plate 4) were related to each other. A number of oil and gas fields surround this structure but the structure itself has not been extensively tested.

Northwestern Area

Nearly all of the data available in the northwestern area, T29-30N, R3W, were shot by Southland Royalty as part of a single survey. Our interpretation indicates that the nearly orthogonal pattern is still present in all three horizons but has been rotated counterclockwise to N10^{o}-20^{o}W and N60^{o}-80^{o}E. We did not identify any major structures in the area of the survey. Although a small north-striking, west-verging thrust fault in the basement nearly bisects the area, this direction is not reflected in any of the overlying horizons. No fields have been developed in this area but there is significant gas production immediately to the west of the Reservation boundary.

Several southwest-verging thrust faults mark the northeastern margin of the San Juan Basin at the far northwestern corner of the Reservation. The largest of these displaces the top of basement approximately 825 m (2700 ft) vertically and 3 km (1.8 mi) into the basin. The highest strata affected by this fault are in the lower part of the Cretaceous section. A large northwest trending and southwest facing monocline overlies this fault zone.

Northeastern Area

The northeastern area, T27-28N, R1E-2W, is the most highly faulted part of the Reservation studied in this project. Nearly all of the data available from this area were acquired by American Hunter in a multiyear program. Shooting parameters for the American Hunter data resulted in 30 to 60 fold, and were acquired between 1991 and 1993 in a well laid out grid pattern. All of the lines were processed and displayed alike, greatly facilitating the interpretation. Parts of the survey are over existing oil fields so there is reasonable well control for the seismic data.

A number of north-south trending, west-verging and east-verging thrust faults underlie the eastern part of this area, some traceable nearly to the surface. A north-south trending west facing monocline overlies this fault zone and the Mesaverde and Pictured Cliffs horizons are extensively faulted in both the north-south and east-west directions in the vicinity. The Puerto Chiquito and Boulder oil fields produce from fractured Mancos Shale on or adjacent to this structure.

Conclusions and Recommendations

Several factors influence the patterns of faulting displayed on plates 2, 3, and 4. The orientation of the two-dimensional seismic lines tend to influence how faults can be drawn. Using only two-dimensional data limits the interpreters to constructing straight line fault segments. In reality almost all faults have a curved pattern that trends in a straight line. Others factors influencing the result are geologic in nature and are a product of the evolution and tectonics of the region. As previously mentioned, we confined ourselves to straight-line fault segments except in certain circumstances. We realize this is undoubtedly not the case in the real world but felt it was the only practical way to deal with the almost unlimited correlation possibilities in much of the area. The major exceptions to this rule are the thrust faults in the northeastern area. We felt justified in using curved lines in these cases because of the uniqueness and reasonably constant number of these faults. The geometry of this grid also increases our confidence in the fault interpretation.

A second factor that may have partly biased our interpretations is the geometry of the seismic surveys themselves. We cannot estimate how much of a factor this might be except to say that we were cognizant of the possibility and continually tested the data with other directions. Alternatively, it should be noted that most of these surveys took advantage of existing roads and topography wherever possible rather than going cross-country with a purely geometric grid. Previous work has demonstrated the control exerted on present topography by underlying fault and joint patterns in the San Juan Basin so we feel it likely that the geometry of the surveys was strongly influenced by local fault and fracture directions. Moreover, much of this area had already been explored to some extent before these data were acquired so it is probable that something was already known about the structural trends when the surveys were planned. Consequently, many of the lines are at high angles to the structure and others nearly parallel.

A general observation that can be made from the fault patterns is that the closer one approaches the basin margin the more nearly the fault trends approximate the trend of the bounding structures. Wherever we have been able to observe the structure of the basin margin along the eastern, northern, and western sides we have found thrust faults indicating Laramide age basinward compression or transpression. The direct effects of this deformation disappear into the basin but along the margins they can be significant. In the area of the Jicarilla Reservation this influence is striking. If this apparent relationship remains consistent, we would expect the fault directions north of the American Hunter survey to bend to the northwest into approximate parallelism with those interpreted in the Southland Royalty survey. Likewise, north of the Southland Royalty survey we would expect them to continue swinging northwestward to parallel the thrust faults in the northwestern corner of the Reservation.

The zone of thrust faulting in the northeastern area lies approximately along the trend of the Nacimiento Fault to the south. Baltz (1967) described the Nacimiento Fault as a Laramide high angle reverse fault with some demonstrable right lateral movement. We interpret the zone of thrust faulting to be the northern limit of the Nacimiento Fault. A possible interpretation of the fault geometry would be that the thrusts and backthrusts form a positive flower structure suggesting the presence of lateral movement on an underlying fault (figure 17). The amount of lateral movement would not be great because no offset is apparent on magnetic and gravity data in the area (Cordell and Keller, 1984) but could still be enough to form an area of transpression as the lateral movement is distributed among several faults. An alternative interpretation would not involve any lateral movement, relating the thrust faulting to compression from the east instead (figure 18). An unambiguous solution is impossible without seismic data in the intervening areas.

Regardless of the ultimate cause for the thrust faulting, the result is that the overlying rocks are highly fractured and even offset in places. We think it probable that these effects will decrease to the north but have no evidence to indicate what the geometry of the overlying structure might be as the thrusting either dies out or changes direction. This area likely contains a significant number of structural traps for hydrocarbons but an analysis of the open fracture directions and a detailed analysis of the faulting using 3-D seismic will be necessary to locate them.

Another major influence on the fault patterns and open fracture directions is the close proximity of the Jicarilla Reservation to the Rio Grande Rift and the related extensional deformation. The north to northeast direction of the rift segments closest to the Reservation suggest that these fault and fracture directions most likely exhibit tensional features and be open. The presence of a significant number of identifiable NS-trending faults in the Mesaverde and Pictured Cliffs horizons along the eastern parts of the Reservation may to a large degree, reflect the influence of the rifting since the associated extension would have caused normal offset on a number of these faults.

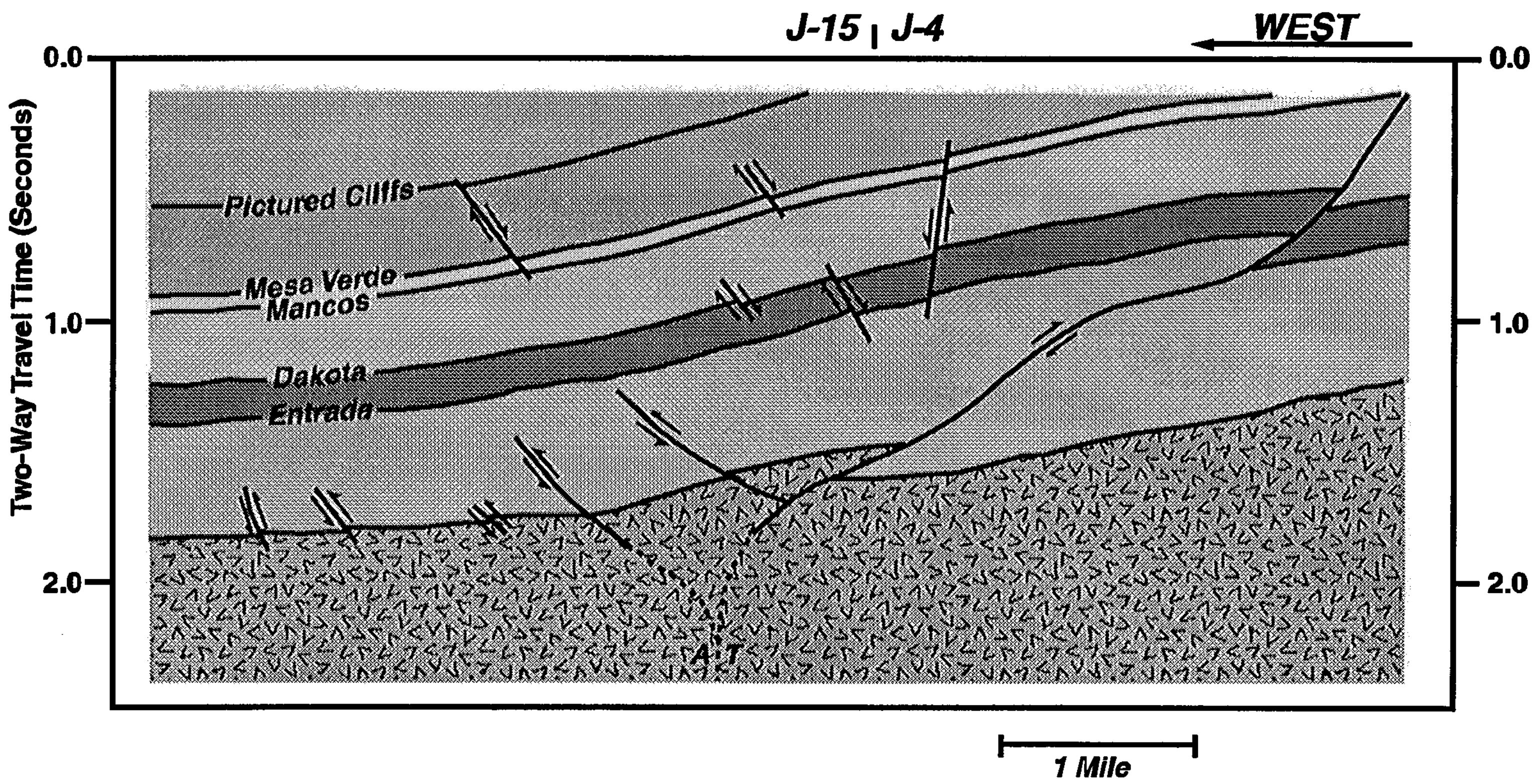

Figure 17. Line drawing interpretation of American Hunter line J-15 and J-4, Jicarilla Indian Reservation showing transpression and possible flower structure over right-lateral wrench fault.

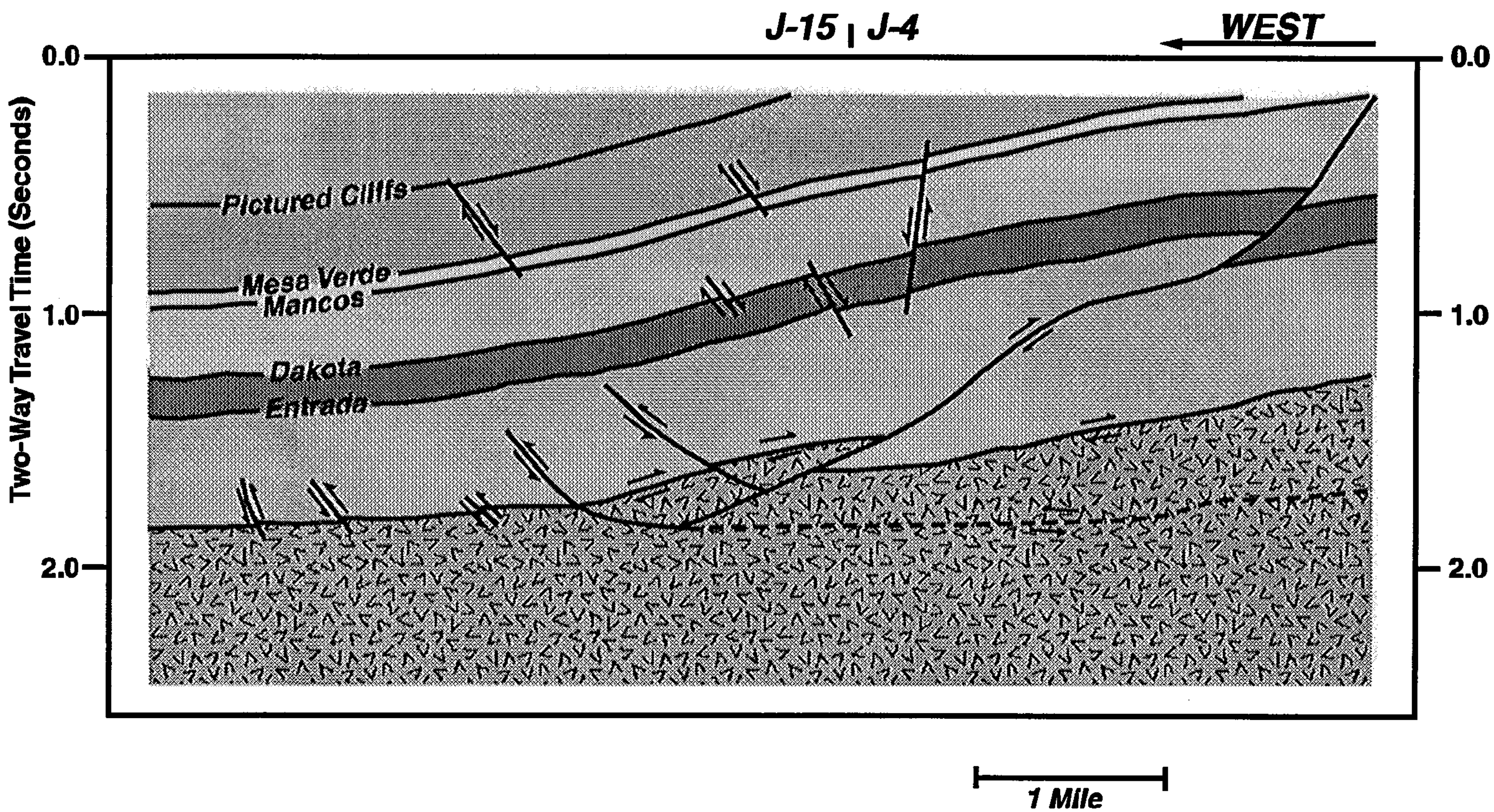

Figure 18. Line drawing interpretation of American Hunter composite line J-15 and J-4 Jicarilla Apache Indian Reervation showing compression with no lateral movement.

This study has not only revealed several prospective areas for hydrocarbon exploration on the Jicarilla Reservation but it has also helped to explain some of the underlying causes for the observed structural patterns. Structures such as the structural high along the southern Reservation boundary and the monocline along the northeastern boundary can be related to basement structures and explained, at least in the case of the monocline, in terms of basin evolution and regional tectonics.

Among the conclusions that may be drawn from this study, the most important to the search for additional hydrocarbon resources on the Jicarilla Reservation is the documentation of the relationship of structures in the potential reservoir rocks to those in the basement and around the margins of the San Juan Basin. The recognition of three structural provinces within the Reservation and the approximate parallelism of structures to the adjacent basin margin provide predictive tools for future exploration and development. Furthermore, the proximity of the Reservation to the Rio Grande Rift suggests that north and slightly northeast trending faults and fractures should be open and provide conduits for fluid migration.

We have noted several areas where additional drilling and geophysical investigations would significantly enhance the prospects for hydrocarbon discoveries on the Jicarilla Reservation. In addition to those areas on the Reservation, we strongly recommend that any future studies also include some of the critical adjacent areas, especially those immediately to the east and south. We also recommend that any future studies include some 3-D seismic surveys in the most critical areas. At the very least, an effort should be made to obtain the digital data for all of the seismic surveys on the Reservation. Some of this will need to be in the form of field tapes and observer's notes so that the data may be reprocessed and then converted to depth and mapped. Without this type of conformity it will be very difficult to use the seismic data to produce the sort of maps or stratigraphic analyses necessary to take the next step in developing the hydrocarbon resources on the Reservation.

References Cited

Baltz, E.H., 1967, Stratigraphy and regional tectonic implications of part of Upper Cretaceous and Tertiary rocks east-central San Juan Basin New Mexico: U. S. Geological Survey Professional Paper 552, 101 p.

Cordell, L., and Keller, G.R., 1984, Regional structural trends inferred from gravity and aeromagnetic data in the New Mexico-Colorado border region, *in* Baldridge, W.S., Dickerson, P.W., Riecker, R.E., and Zidek,J., eds., Rio Grande Rift—northern New Mexico: New Mexico Geological Society Guidebook, p. 21-23.

Sheriff, R.E, 1989, Encyclopedic Dictionary of Exploration Geophysics – second edition; Society of Exploration Geophysicists, 323 pages.

Taylor, D.J., and Huffman, A.C., Jr., 1998, Map showing inferred and mapped basement faults, San Juan Basin and vicinity, New Mexico and Colorado: U.S. Geological Survey Geologic Investigation Series I-2641, scale: 1:500,000.

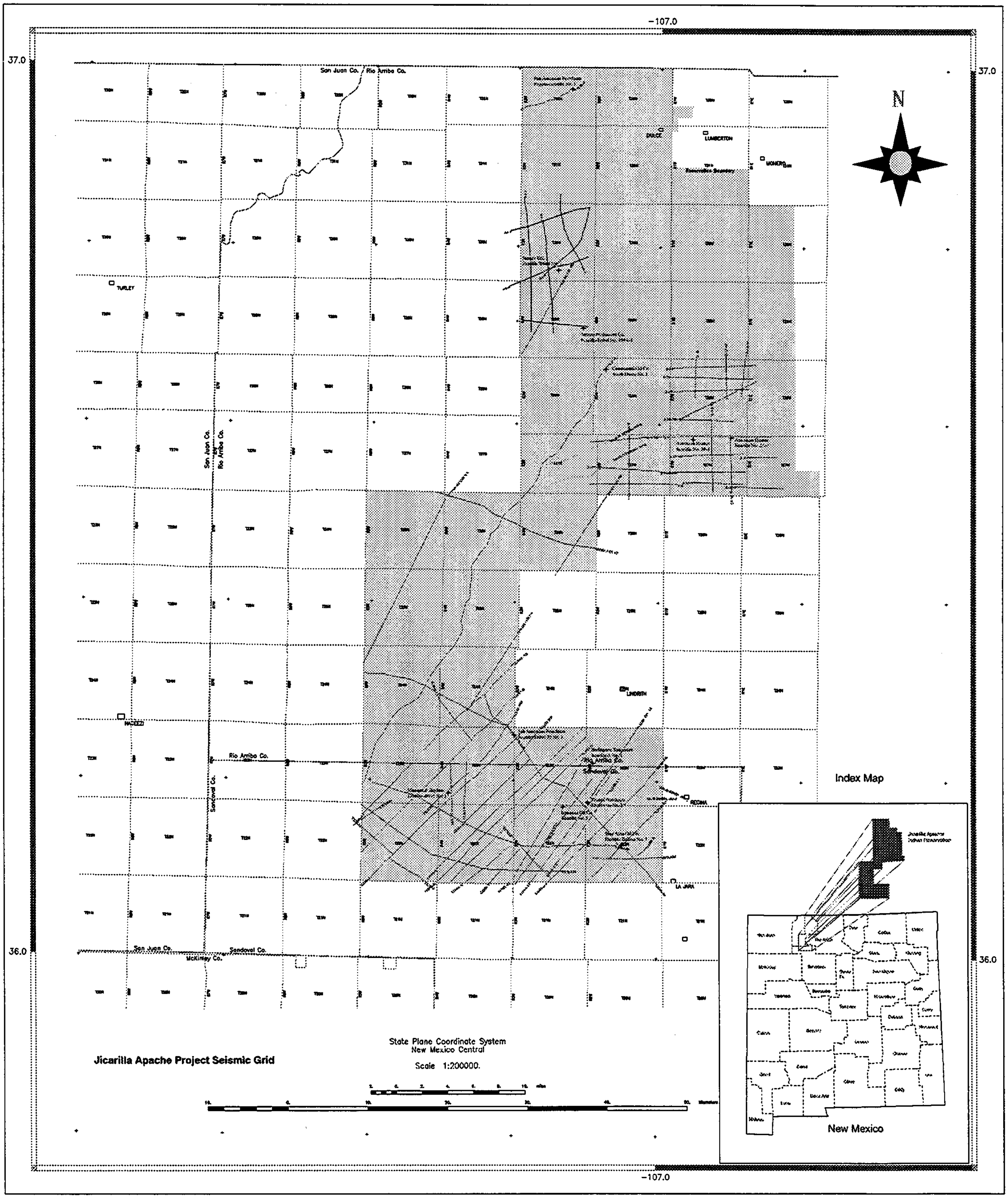

Plate 1. Map of the Jicarilla Apache Indian Reservation study area showing the location for all of the available multichannel seismic reflection data and key wells used in the project

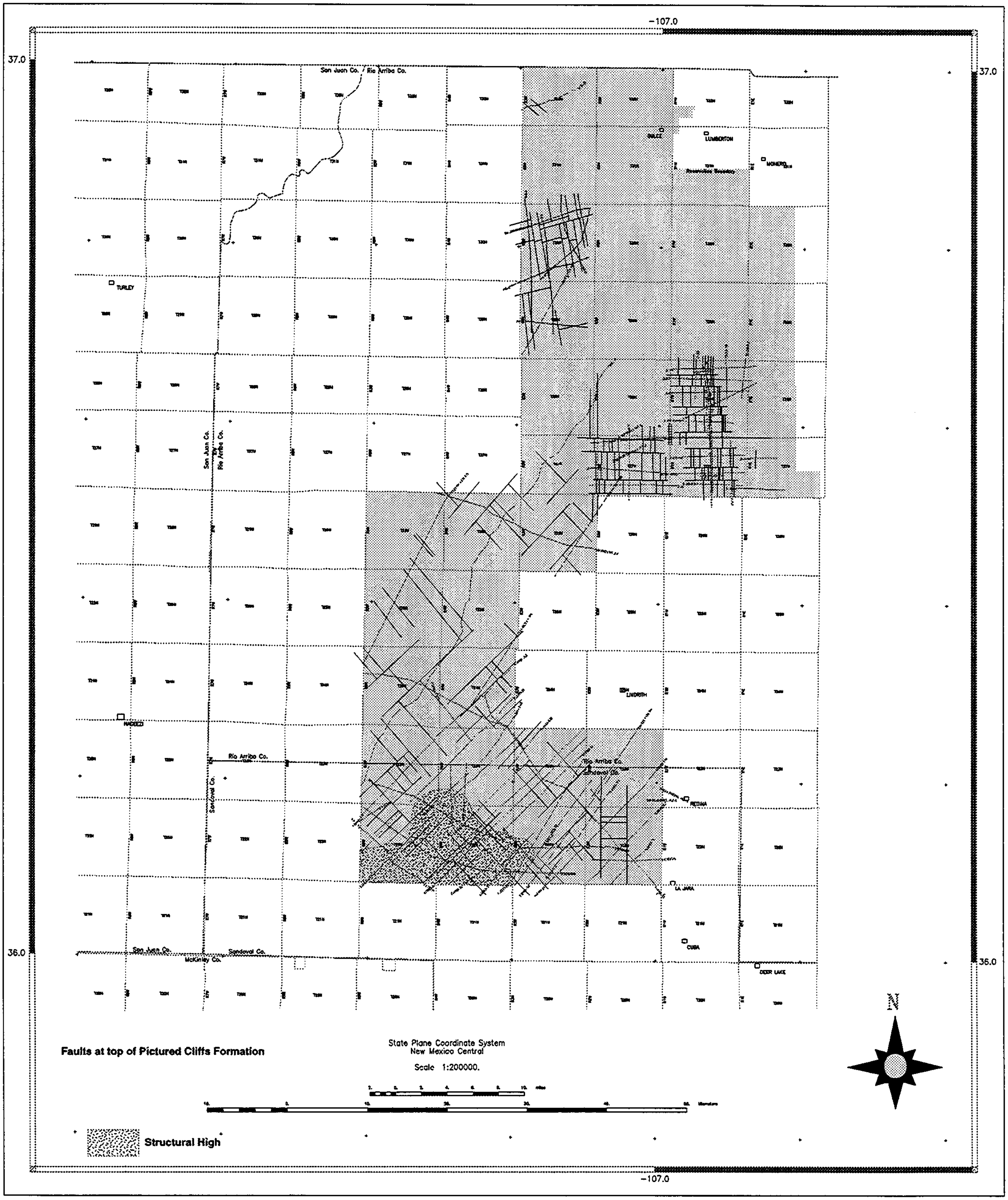

Plate 2. Preliminary map of the Jicarilla Apache Indian Reservation study area showing inferred and mapped faults at the Pictured Cliffs horizon.

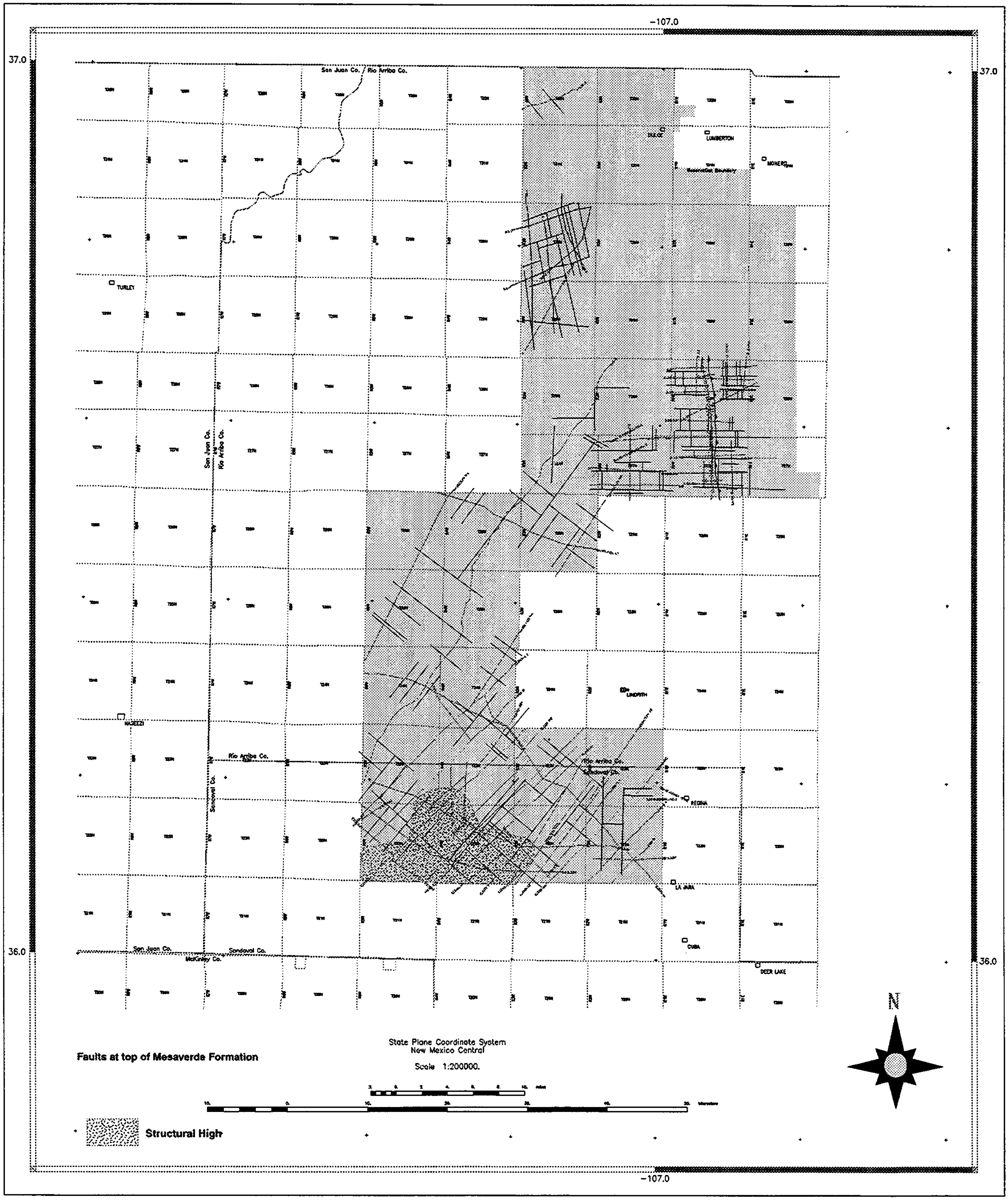

Plate 3. Preliminary map of the Jicarilla Apache Indian Reservation study area showing inferred and mapped faults at the Mesaverde horizon.

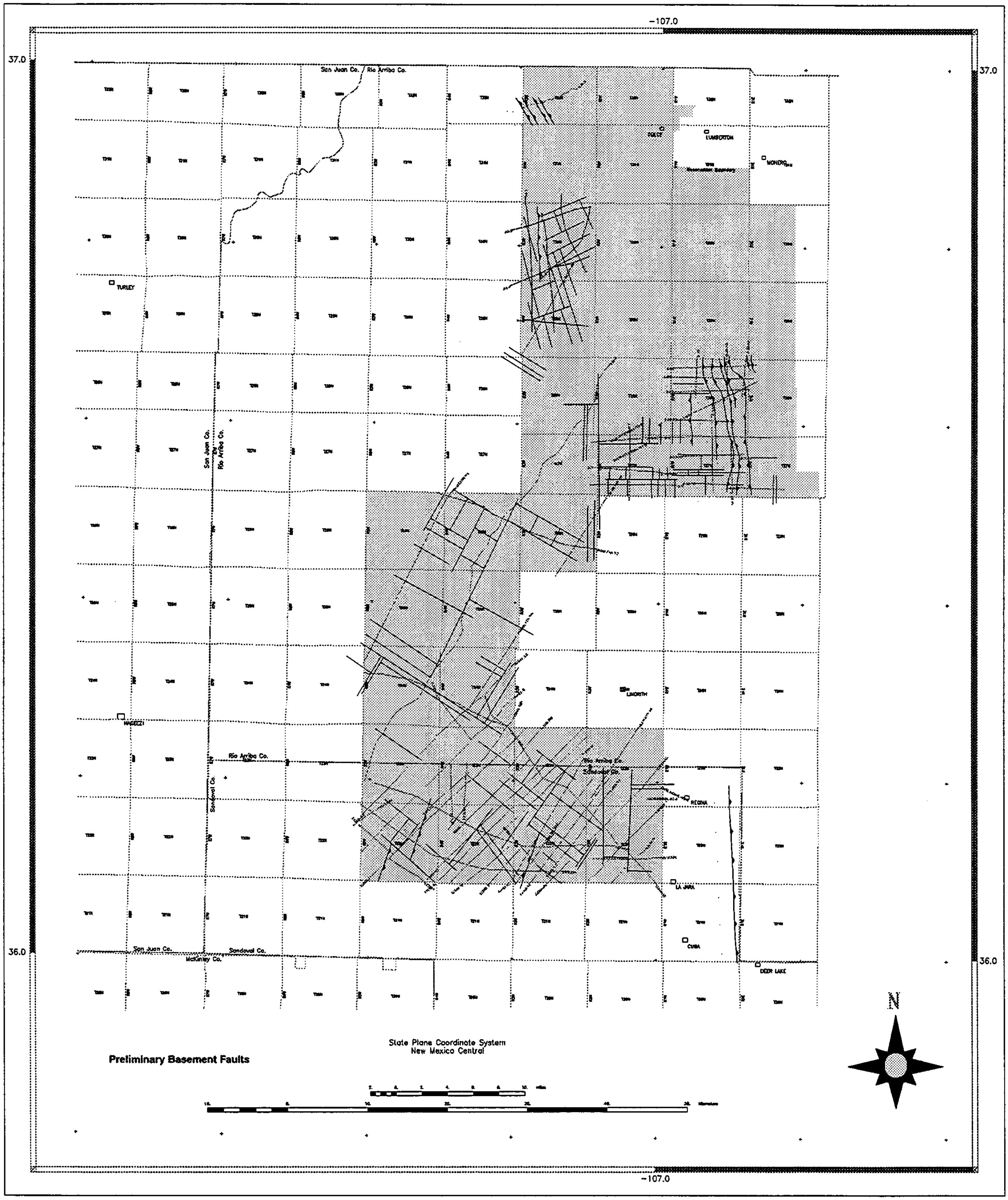

Plate 4. Map of the Jicarilla Apache Indian Reservation study area showing preliminary inferred and mapped faults at the top of the basement.